UNIVERSITAT ROVIRA i VIRGILI

3D-printable materials with vitrimer-like behavior based on disulfide dynamic bond exchange

FINAL DEGREE PROJECT

Chemistry Degree

Student: Anna Vilanova Pérez

UPC Supervisor: Dr Xavier Fernández Francos

URV Supervisor: Dr. Omar Boutureira Martín

Year 2021/2022

INDEX

1 GLOSSARY

1-MI	1-Methyllimidazole
3D	Three-dimensional
Az	Azelaic acid
AzMA	Monomer prepared from Az and GMA
BAPO	Phenylbis(2,4,6-trimethylbenzoyl)phosphine oxide
BDMA	N,N-Dimethylbenzylamine
$CDCl_3$	Chloroform-d
CLIP	Continuous líquid interface polymerization
^{13}C-NMR	Carbon nuclear magnetic resonance
DBN	1,5-Diazabicyclo(4.3.0)non-5-ene
DMSO	Dimetyl sulfoxide
DIW	Direct-ink-writing
DLP	Digital light processing
DMA	Dynamic mechanica analysis
DMAP	4-(Dimethylamino)pyridine
DSC	Differential scanning calorimetry
FEMA	Ethylene glycol phenyl ether methacrylate
FTIR	Fourier transform infrared spectroscopy
GMA	Glycidyl methacrylate
HEA	2-Hydroxyethyl acrylate
HEMA	2- Hydroxyethyl methacrylate
^{1}H-NMR	Proton nuclear magnetic resonance
IMA	Isobornyl methacrylate
LUP	1,1-Bis(tert-amylperoxy)cyclohexane solution
PEGMA	Poly(ethylene glycol) methyl ether methacrylate
S2	4,4'-Dithiodibutyric acid
S2P	3,3'-Dithiodipropionic acid
S2PMA	Monomer prepared from S2P and GMA
S2MA	Monomer prepared from S2 and GMA
TBD	1,5,7-Triazabicyclo(4.4.0)dec-5-ene
TBP	Tributylphosphine
TEA	Triethanolamine
TEMPO	Tetramethylpiperidinooxy
TEYA	Triethylamine

T_g	Glass transition temperature
TGA	Thermogravimetric analysis
TPO	Diphenyl(2,4,6-trimethylbenzoyl) phosphine oxide
TPP	Triphenylphosphine
UV	Ultraviolet

2 SUMMARY

In this project, a new family of vitrimeric materials based on the dynamic exchange of disulfide linkages has been developed.

Two different monomers have been synthesized, one that contains sulfur-sulfur linkages and the other one without has been used as a reference. Both were characterized using different analytical techniques such as ^{1}H-NMR and FTIR.

A set of samples with different formulations have been analysed in order to achieve an appropriate catalytic system which selectively activates the disulfide bond exchange. After evaluating the thermal-mechanical properties of each material and their vitrimeric capabilities using thermal analytical techniques such as DSC, DMA and TGA, among others, a final formulation was chosen. The material was tested in the 3D printer, and its repairing and reprocessing capabilities were evaluated.

Finally, it has been proposed possible further alternatives to solve the main problems arised in our work.

RESUM

En el present treball hem desenvolupat, una nova família de materials vitrimerics basats en el intercanvi dinàmic del enllaç S-S.

S'han sitetitzat dos monòmers diferents, un que contenia enllaços S-S i l'altre sense, el qual va ser emprat com a referencia. Ambdós es van caracteritzar utilitzant diferents tècniques analítiques com ara ^{1}H-RMN and FTIR.

S'han analitzat tot un seguit de mostres amb diferents formulacions per tal d'aconseguir un sistema catalític apropiat que activi selectivament el bescanvi S-S. Un cop avaluades del propietats termomecàniques de cada material i les seves propietats vitrimeriques utilitzant tècniques calorimètriques com DSC, DMA and TGA, entre d'altres, es va escollit finalment una formulació. Aquesta va ser assajada en una impressora 3D, avaluant seguidament les propietats del material final en quant a capacitat per ser reparat i reciclat.

Per acabar, s'han proposat possibles vies per continuar la investigación per tal de solucionar els problemes més rellevants que ens vam trovar al llarg de la nostra recerca.

3 OBJECTIVES

The main objective of this work is developing a 3D-printable material having dynamic covalent bonds, providing the material with a crosslinked structure and a vitrimeric behaviour, based on dynamic exchange of disulfide linkages. Printed parts could therefore be repaired, recycled and reprocessed.

Two monomers will be synthesized in the first place, one that contains sulfur-sulfur linkages and the other one without them which will be used as a reference.

In order to activate selectively the disulfide bond exchange it is required to find out an appropriate catalytic system. Materials containing the different monomers and catalytic systems will therefore be studied.

A set of analytical techniques will be used to determine the thermal-mechanical properties of the material and evaluate its vitrimeric capabilities. Thermal analytical techniques such as DSC, DMA and TGA, among others, will be used.

Once a candidate formulation has been selected, it will be tested in the 3D printer and repair-reprocessing capabilities will be evaluated.

4 INTRODUCTION

4.1 Background

The research group at the Thermodynamics Laboratory (Heat Engines Department) from the ETSEIB (UPC) has carried out an intense research labour in the field of thermosetting polymers for the last 20 years in collaboration with the FUNCMAT group of the Department of Analytical and Organic Chemistry from the Universitat Rovira i Virgili (URV). Research focuses on the processing and characterization of novel thermosetting materials with optimum thermal-mechanical properties by means of calorimetric, thermomechanical, imaging and spectroscopic techniques, among others.

Currently, the research group from ETSEIB is working on active network polymers and its applications in 3D printers. This project has been developed within this context.

Thermosetting polymers

Polymers can be categorized in two main groups depending on its thermal behaviour: thermoplastics and thermosets. The last ones could be defined as polymer that have a covalent three-dimensional networking structure which normally provides the material excellent thermomechanical properties and excellent chemical resistance. This network is formed due to an irreversible reaction and for that reason they cannot be reshaped, processed, or recycled. Typical examples of thermosetting polymers are phenolic and urea-formaldehyde resins, unsaturated polyesters, and epoxy resins.[1]

Thermosetting polymers are usually obtained after the polymerization reaction of monomers, oligomers or mixtures of them, triggered by the application of heat or UV light, and with the help of adequate initiators or catalysts. During this process, illustrated in Figure 1, this liquid-like mixture transforms into a non-flowing crosslinked network structure.[1]

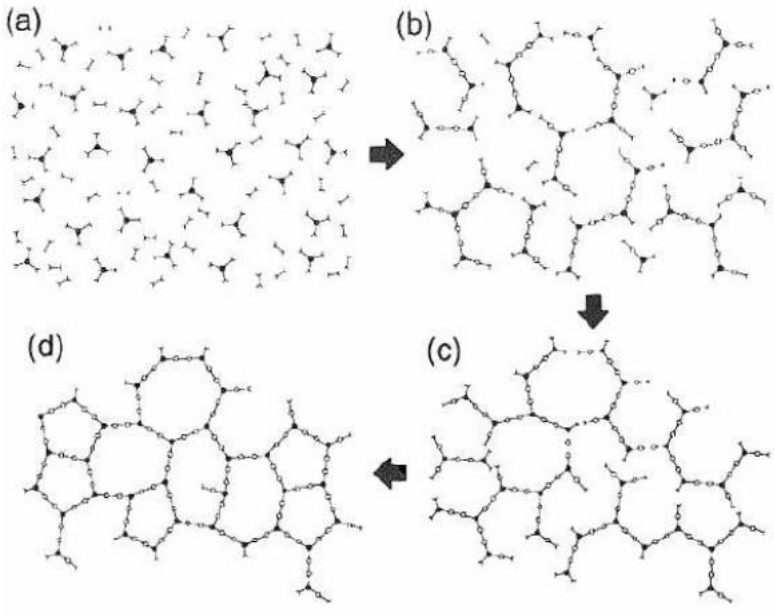

Figure 1: Formation of a thermosetting polymer network: (a) mixture of monomers, (b) polymer chain growth and branching, (c) gelation and (d) crosslinked network. Adapted from [1]

An important characteristic that should be considered is the glass transition temperature (T_g). This temperature represents the transition from a rigid, glassy state to a rubbery state for both, thermoplastic (amorphous fraction) and thermosetting polymers. Glass temperature is determined using techniques as differential scanning calorimetry (DSC) or dynamomechanical analysis (DMA).[1]

The T_g is a relevant parameter in the processing of thermosets. The starting monomers have a very low glass transition temperature (T_{g0}) and, when the curing process starts, the T_g of the system increases due to the decrease in free-volume caused by the formation of new covalent bonds and the restrictions to chain mobility imposed by the increasing degree of crosslinking once gelation has taken place. When T_g is comparable to the cure T a reversible transformation called vitrification could occur. If this happens the reaction can be incomplete, and the material would not have the desired properties.[1]

To overcome this effect, the reaction process should be completed in an additional step at temperature higher than the ultimate glass transition of the material, $T_{g\infty}$ [1]. Figure 2 graphically shows the phenomenological behavior of the formulation during curing as a Time-Temperature-Transformation diagram.

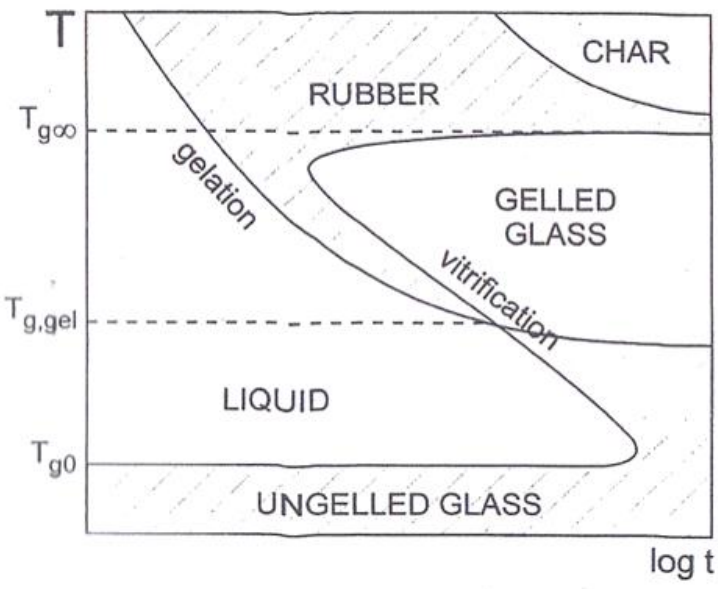

Figure 2: Time-temperature transformation (TTT) diagram. Adapted from [1]

3D-printing

Recent applications of thermosets include their processing using 3D printing techniques, with the purpose of producing objects with geometric features difficult to achieve using other conventional techniques. The main technologies available for the 3D-printing of thermosets are:

- **DIW (Direct-ink-writing):** A thick mixture of monomers and fillers is extruded out through a nozzle attached to a syringe and subsequently cured using a light source. This process resembles the well-known fused deposition modelling (FDM) technique widely used for thermoplastics.[2]
- **DLP (Digital light processing):** A liquid mixture of monomers, placed inside a vat or vessel, is polymerized layer-by-layer by masked image projection, each layer all at once, using a UV-light projector. It is an evolution of stereolithography (SLA) where a laser beam scans the surface and photocures the resin.[2]

- **CLIP (Continuous liquid interface):** This is an evolution of the DLP technology, based on the use of a vat with an oxygen-permeable window, making it possible to print objects in a much faster way due to the formation of a dead zone at the bottom of the vat where the diffusion of oxygen prevents polymerization, so that the printed object does not have to be detached from the vat every layer.[3]

Specifically, in DLP, two main polymerization systems are used: (a) cationic ring-opening polymerization of epoxides and other cyclic ethers and (b) radical polymerization of acrylates and methacrylates.[4] This project focus in the second type which is also the most used in the industry. It is known that acrylates are generally more reactive than methacrylates. In order to obtain a crosslinked material, the mixture of (meth)acrylates used must contain at least a component bearing 2 or more (meth)acrylate groups.[1]

The photopolymerization of (meth)acrylates requires the use of photoinitiator (PI). PI's absorb light in the UV-visible spectral range then rise to an electronical excited state, by promotion of an electron a higher-energy orbital. Subsequently, the light energy convers into chemical energy in the form of reactive intermediates, in this case free-radicals, that initiates polymerization on monomers. The reaction mechanism is complex but can be summarized in the set of reaction steps shown in Figure 3.

$PI \rightarrow R^* (h\nu)$	Formation of initiating radical
$R^* + M \rightarrow RM^*$	Initiation
$RM^* + nM \rightarrow RM_{n+1^*}$	Propagation
$R(M)_{n^*} + R(M)_{m^*} \rightarrow R(M)_n - R(M)_m R$	Termination (coupling)
$R(M)_{n^*} + R(M)_{m^*} \rightarrow R(M)_n - H + R(M)_{m-1} M_{-H}$	Termination (disproportionation)

Figure 3: Scheme of the photopolymerization of (meth)acrylares

Vitrimer

In 2011 a new category of materials was defined, called vitrimer, made of covalently bound chains.[5], [6] This is a particular class of dynamic networks, in which the materials are able to rearrange their network structure by the activation of dynamic covalent bond exchange reactions under various stimuli, including heat, light and pH.[7] Vitrimers show a typical thermoset behaviour at low temperatures, but at high temperatures they behave like melted glass, without losing the integrity of their network structure, making possible their reshaping, repairing, processing and recycling, in a similar way to thermoplastic materials.[6]

Dynamic covalent bond exchange can be divided into two groups, depending on their exchange mechanism:

- **Dissociative:** Where an existing bond is broken before a new bond is formed.
- **Associative:** Where the cleavage of the existing bond and the formation of new one is concerted.

The term vitrimer only applies to the second mechanism.

Inside vitrimer materials some subdivisions could be found based on the nature of the dynamic exchange reaction.[6]

- **Carboxylate transesterification:** The most studied reaction, performed by a carboxylic acid-base transesterification reaction, promoted by a catalyst.

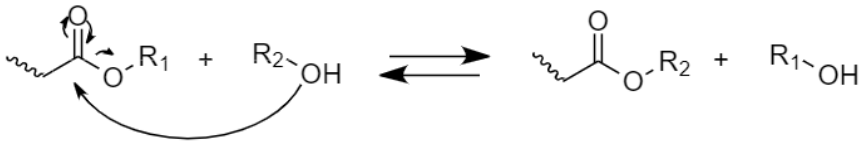

Scheme 1: Carboxylate transesterification mechanism

- **Transamination of vinylogous urethanes:** The reaction works like Michael addition, where an activated double bond is attacked by an amine group. It is carried out without catalyst.

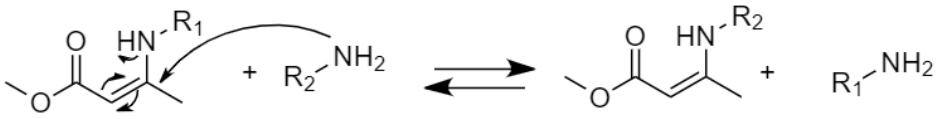

Scheme 2: Transamination of vinylogous urethanes mechanism

- **Disulfide exchange chemistry:** The behaviour of covalent exchange disulfide bonds is complex, since it involves several mechanisms.[8] Three examples would be:

    - ***Thiol-disulfide exchange:*** Involves the nucleophilic displacement of a thiolate anion from the disulfide, through attack to another thiolate anion. This process is catalyzed by bases.
    - ***Disulfide exchange:*** can be activated under UV-light or moderate temperatures along with base catalysts or nucleophiles, typically ternary amines or phosphines.
    - ***Aromatic disulfide exchange mechanism:*** it is proposed that goes through radical-mediated [2+1] mechanism.

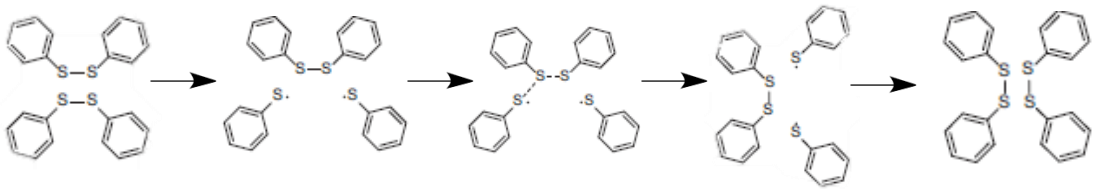

Scheme 3: Aromatic disulfide exchange mechanism

Other examples could be transalkynation of tiazolium salts, olefin metathesis and imine amine exchange reaction among others[6].

4.2 Project definition / objectives

This study will first focus on the development of vitrimers that contain disulfide linkages which can carry out the disulfide bond exchange reaction, catalysed by bases and phosphines.[9], [10]The effect of different catalysts on the disulfide exchange and the overlapping of other dynamic bond exchange processes such as transesterification will be studied.

Apart from the study of this family of vitrimers, this project has a second part which would be introduced the vitrimer into a 3D-printable ink in order to create pieces with a particular shape, repair and recycle them. A typical recycling process for this type of materials would consist in grinding the piece and applying a thermal compression moulding to produce an object with a different application.

By the time this project was started, very few studies about vitrimers with disulfide bonds used in 3D printers which have thermosetting properties had been found in the lliterature, for instance the printing of polyurethane elastomers with disulfide bonds[11]. In contrast, we found several reports about 3D-printed vitrimers based on transesterification, with recycling capabilities and minimal loss of thermomechanical properties.[2], [12]–[14]

Different disulfide structures can be used in thermoset applications. Dynamic exchange of aromatic disulfides can take place at room temperature in the absence of catalyst, but their incorporation into 3D-printable formulations is unfeasible because the dynamic exchange produces radicals that would trigger the (meth)acrylate polymerization.[7], [8] Materials can be reshaped and recycled at room temperature or higher temperature depending on the mobility of the network.[7], [8], [15]

Taking everything into account, the next experiment was designed.

Two monomers with similar structures were synthetized, one containing sulfur-sulfur linkages (S2MA) and the other without (AzMA), which will be used as a reference. The formation of these different monomers is shown in Scheme 4.

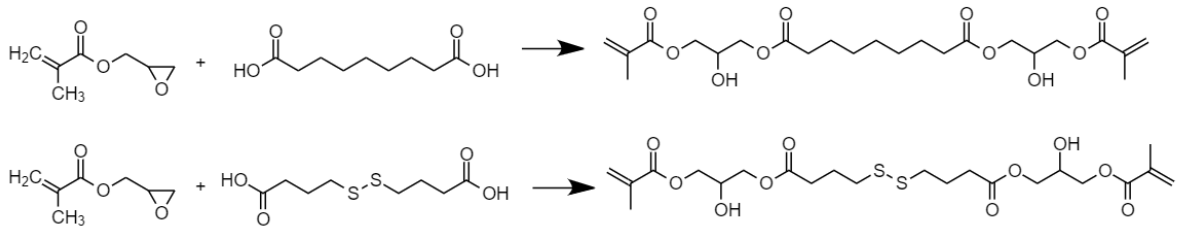

Scheme 4: Synthesis of S2MA (upper scheme) and AzMA (lower scheme).

S2MA and AzMA are tetrafunctional crosslinking monomers (2 group acrylic per molecule). They will be incorporated into formulations in combination with other mono (meth)acrylate co-monomers, so that no other crosslinks are formed in the network structure.

A radical photoinitiator is required for the activation of the radical polymerization process, such as Phenylbis(2,4,6-trimethylbenzoyl) phosphine oxide (BAPO) and Diphenyl(2,4,6-trimethylbenzoyl) phosphine oxide (TPO)[12]. The formulation should also include catalysts that promote the disulfide bond exchange reaction, typically phosphines and/or tertiary amines[7], [9], [16]

5 EXPERIMENTAL

5.1 Materials

Preparation of monomers

Two dimethacrylate monomers were prepared in the first place, one contains sulfur-sulfur linkages (S2MA) and the other without (AzMA) as it will be used as a reference. The structure of these two monomers is shown in Figure 4.

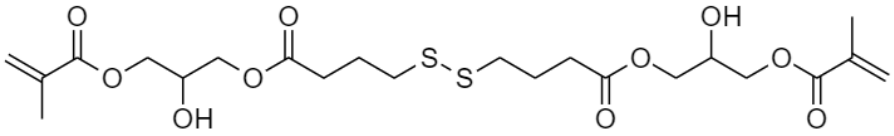

S2MA

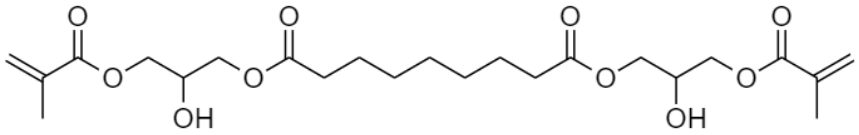

AzMA

Figure 4: Structure of the S2MA and AzMA dimethacrylate monomers prepared.

Table 1 shows the different reagents used for the preparation of S2MA and AzMA monomers, the molecular weight, the purity, their acronyms, and a little description about its role into the reaction. Their structure appears in Figure 5. All the material required for the synthesis of monomers have been supplied by Sigma-Aldrich and used without further purification.

*Table 1: Reagents employed in the preparation of the methacrylate monomers and main characteristics. *Purity minimum required according to the specifications.*

Name	Acronym	Molecular weight (g/mol)	Purity*	Description
Azelaic acid	Az	188,22	98%	Reagent
4,4'-Dithiodibutyric acid	S2	238,32	95%	Reagent
Glycidyl methacrylate	GMA	142,15	97%	Reagent
Tetramethylpiperidinooxy	TEMPO	156,25	98%	Radical scavenger
Triethanolamine	TEA	149,19	98%	Catalyst

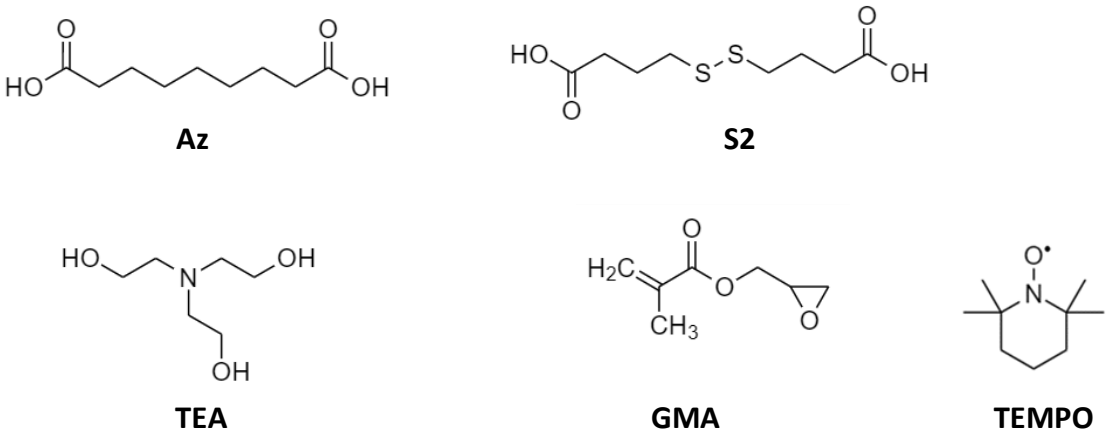

Figure 5: Structure of the reagents employed in the preparation of the methacrylate monomers.

Preparation of formulations

Table 2 shows the molecular weight, the purity, their acronyms, and a little description of the diferent acrylate/methacrylate co-monomers employed in the preparation of the formulations, and their structures are represented in Figure 6. The different initiators and catalysts used are shown in Table 3 and represented in Figure 7. All methacrylate and acrylates monomers, bases and phosphines have been supplied by Sigma-Aldrich. Photoinitiator Diphenyl(2,4,6-trimethylbenzoyl) phosphine oxide (TPO) has been supplied by Ciba Specialty Chemicals Inc and thermal initiator (LUP) has been supplied by Arkema. All the reagents have been used without further purification.

*Table 2: Acrylate and methacrylate co-monomers employed in the preparation of the formulations. *Purity minimum required according to the specifications.*

Name	Acronym	M (g/mol)	Purity*	Description
2-Hydroxyethyl acrylate	HEA	116,12	96%	Acrylate
2- Hydroxyethyl methacrylate	HEMA	130,14	97%	Methacrylate
Poly(ethylene glycol) methyl ether methacrylate	PEGMA	280-320	-	Methacrylate
Isobornyl methacrylate	IMA	222,32	93%	Methacrylate
Ethylene glycol phenyl ether methacrylate	FEMA	206,24	83%	Methacrylate
Diphenyl(2,4,6-trimethylbenzoyl) phosphine oxide	TPO	348,37	97%	Photoinitiator

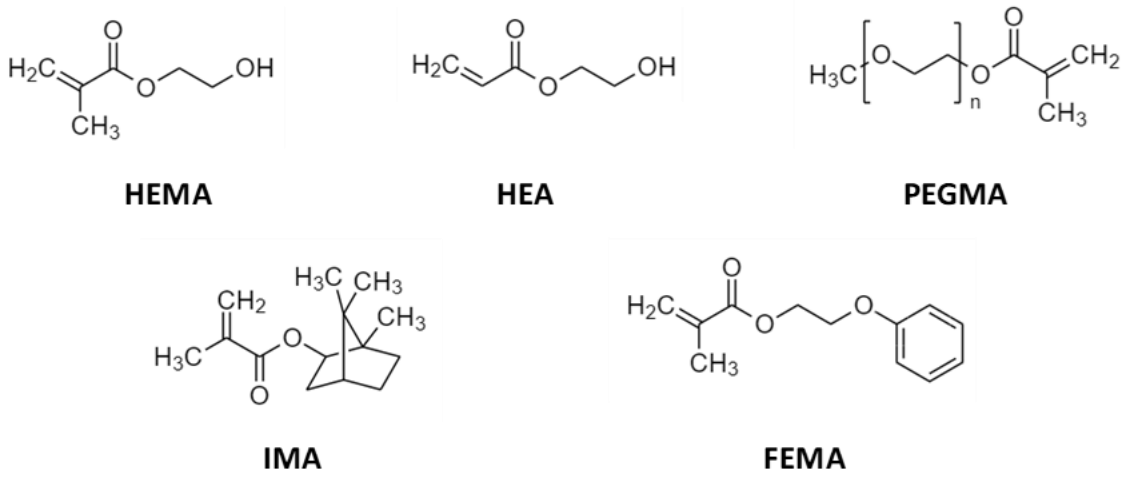

Figure 6: Structure of the acrylate/methacrylate co-monomers employed in the preparation of the formulations.

*Table 3: Initiators and catalysts employed in the preparation of the formulations. *Purity minimum required according to the specifications.*

Name	Acronym	M (g/mol)	Purity*	Description
Diphenyl(2,4,6-trimethylbenzoyl) phosphine oxide	TPO	348,37	97%	Photoinitiator
1,1-Bis(tert-amylperoxy)cyclohexane solution	LUP	288,42	60 wt.% in dodecane	Thermal initiator
Triethanolamine	TEA	149,19	98%	Base
1,5-Diazabicyclo(4.3.0)non-5-ene	DBN	124,18	98%	Base
1-Methylimidazole	1-MI	82,19	99%	Base
N,N-Dimethylbenzylamine	DMBA	135,21	99%	Base
4-(Dimethylamino)pyridine	DMAP	122,17	99%	Base
1,5,7-Triazabicyclo(4.4.0)dec-5-ene	TBD	139,20	98%	Base
Tributylphosphine	TBP	202,32	94%	Phosphine
Triphenylphosphine	TPP	262,29	99%	Phosphine

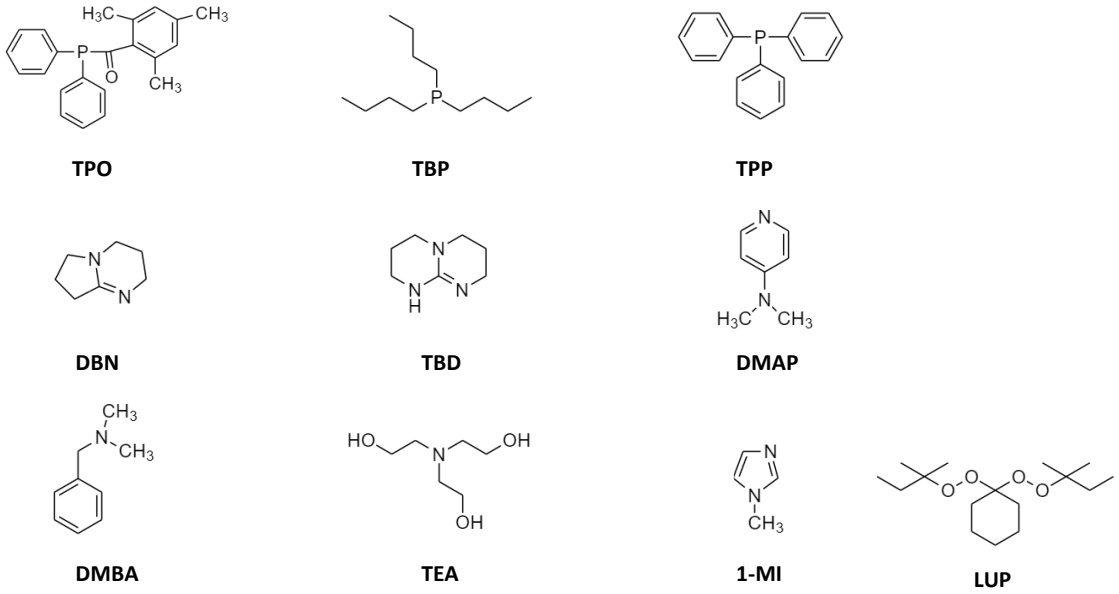

Figure 7: Structure of the initiators and catalysts employed in the preparation of the formulations.

5.2 Preparation of methacrylate monomers

Preparation of S2MA

The main reagents were 4,4'-dithiodibutyric acid (S2) and glycidyl methacrylate (GMA). GMA and S2 were used under stoichiometric conditions (1 epoxy equivalent per acid equivalent). The catalyst (TEA) and the radical scavenger (TEMPO) were added in a proportion of 0.25 wt.% each.

*Table 4: Composition of the formulation for the preparation of S2MA monomer. *Molecular mass*

Name	Equivalents	M (g/eq)	m (g)	% Weight
GMA	1	142,15	142,15	54,13
S2	1	119,16	119,16	45,37
TEA	0,004379	149,19*	0,6533	0,25
TEMPO	0,004181	156,25*	0,6533	0,25

All the reagents were put into a vial and mixed with the help of a spatula. The vial was placed in a silicone oil bath at a temperature of 100 ^{o}C equipped with magnetic stirring. Once complete dissolution of the acid was observed, the vial was removed from the silicon oil bath, wrapped in an aluminium foil and placed again in the bath, now stabilized at 90 ^{o}C, in order to prevent premature activation of the radical polymerization of the methacrylate, leading to gelation. It takes 4 hours to complete the reaction.

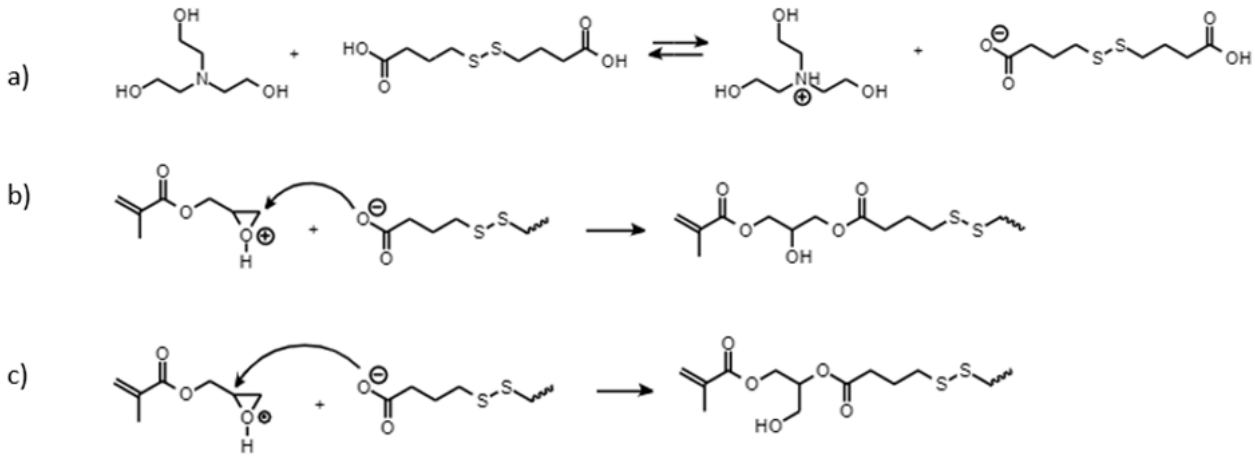

Scheme 5: Proposed reaction mechanism for the preparation of the S2MA monomer: a) acid-base exchange leading to deprotonation of carboxyl group, b) SN2 attack of the carboxylate to the less-substituted carbon of the epoxy ring, c) borderline SN2 attack of the carboxylate to the more substituted carbon of the epoxy ring.

The reaction taking place is the base-catalysed addition of the carboxyl group to the epoxy group (see Scheme 5). The base catalyst is used for the deprotonation of the carboxyl groups leading to a carboxylate anion (Scheme 5.a). The carboxylate anion will either attack the epoxy group by a SN2 reaction to the less substituted carbon of the epoxide leading to a β-hydroxyester (Scheme 5.b) or else by SN2 borderline where the carboxylate anion attacks the more substituted carbon of the epoxide Scheme 5.c). Since the reaction medium is slightly acidic, the epoxy group can be activated by acid protons present, as indicated in the reaction scheme.

The completion of the reaction was verified by Fourier transform infrared spectroscopy (FTIR). The characteristic epoxy peak of the epoxy group from GMA at 908 cm^{-1} (see inset in Figure 8) disappeared completely in S2MA (see inset in Figure 9). It was also observed the appearance of a wide band around 3500cm^{-1} corresponding to de formation of hydroxyl group and a large peak at 1730 cm^{-1} corresponding to carbonyl ester group. The methacrylate double bond peak at 1637 cm^{-1} was unmodified.

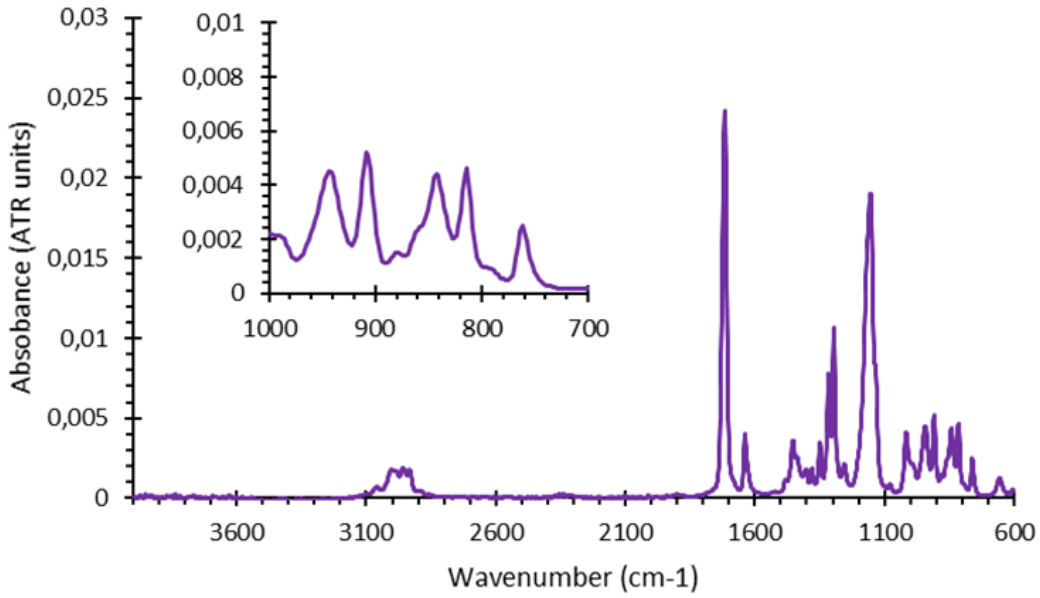

Figure 8: FTIR spectrum of GMA

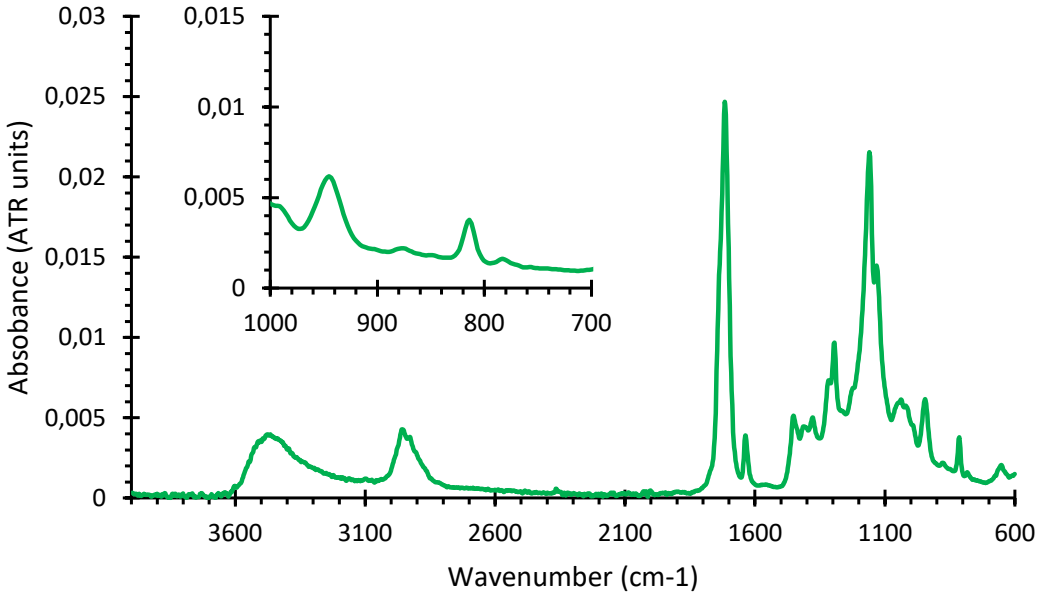

Figure 9: FTIR spectrum of S2MA

To confirm the structure of S2MA, it was analyzed by ^{1}H-NMR. As seen in Figure 10, the main product is the expected one, leading to the formation of a β-hydroxyester (see Scheme 5.b). Nevertheless, the peak at 5.25 ppm (multiplet) also indicates the reaction of the dithiobutyric acid with the more substituted carbon of the epoxide of the glycidyl methacrylate (see Scheme 5.c).

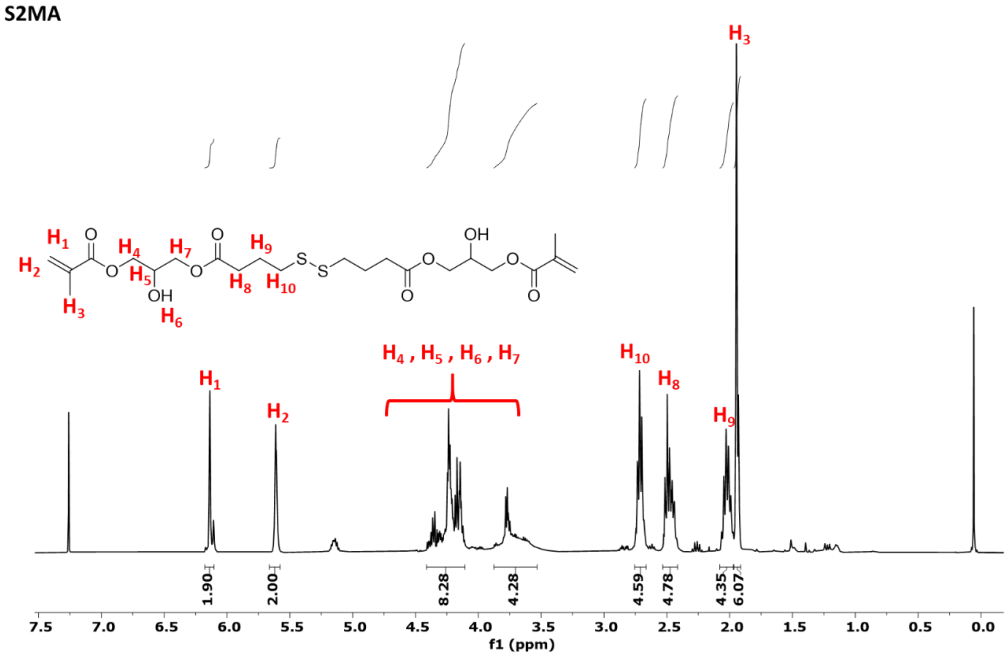

Figure 10: ^{1}H-NMR spectrum of S2MA.

Preparation of AzMA

The main reagents were azelaic acid (Az) and glycidyl methacrylate (GMA). GMA and Az were used under stoiochiometric conditions (1 epoxy equivalent per acid equivalent). The catalyst (TEA) and the radical scavenger (TEMPO) were added in a proportion of 0.25 wt.% each.

*Table 5: Composition of the formulation for the preparation of AzMA monomer. *Molecular mass*

Name	Equivalents	M (g/eq)	m (g)	% Weight
GMA	1	142,15	142,15	59,84
Az	1	94,11	94,11	39,61
TEA	0,004379	149,19*	0,6533	0,28
TEMPO	0,004181	156,25*	0,6533	0,28

The preparation procedure was the same as in the case of S2MA. However, the reaction time needed to be extended up to 8 hours to ensure completion.

To verify the completion of the reaction and the structure, FTIR and ^{1}H-NMR analyses were carried out. The FTIR spectrum (Figure 11) shows that the reaction was not been fully completed since traces of the epoxy group at 908 cm^{-1} were detected. The ^{1}H-NMR spectrum (Figure 12) shows small signals

between 2.5 and 3.25 ppm which correspond to an epoxide group indicating that glycidyl methacrylate is still present in the sample. Moreover, the signal at 5.10 ppm indicates that the by-product formed between azelaic acid and the more substituted carbon of the epoxide of glycidyl methacrylate, is still present in the mixture.

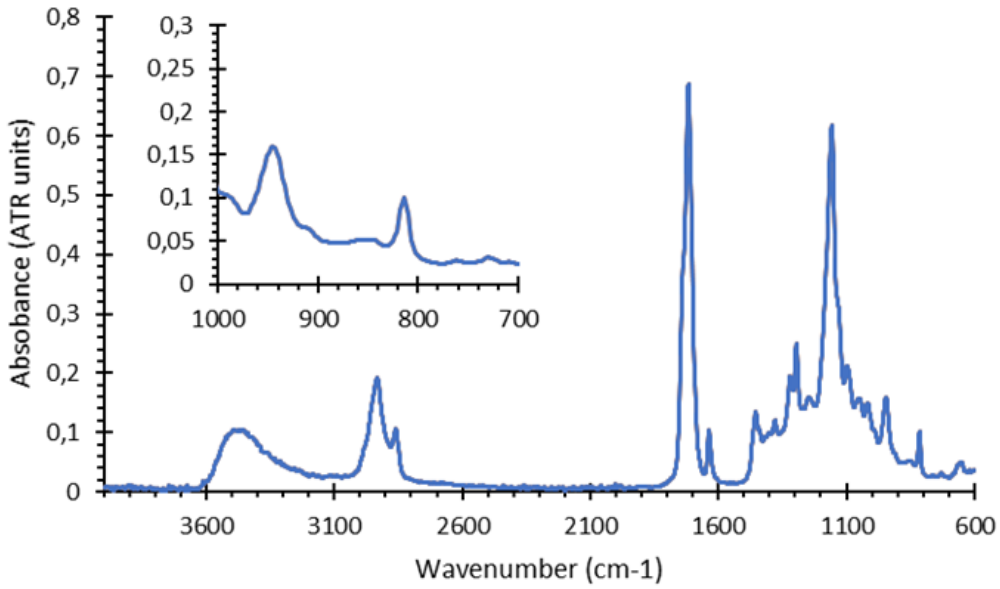

Figure 11: FTIR spectrum of AzMA

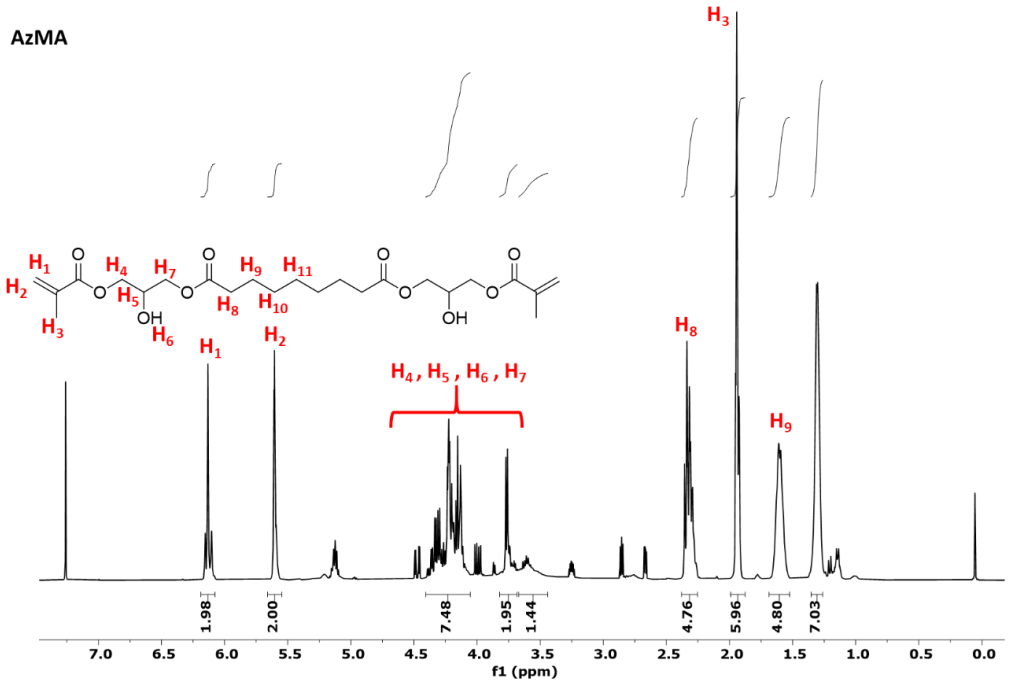

Figure 12: ^{1}H-NMR spectrum of AzMA

5.3 Preparation of formulations and samples

All the formulations were prepared in 5 mL vials. First, all the reagents were introduced with a spatula or a syringe. Then, the mixture was homogenized by mechanical stirring with a spatula.

Formulation used the following nomenclature M-x_C_cat1n_cat2m, where M indicates the dimethacrylate monomer used (S2MA or AzMA), x is the wt.% of the monomer, C is the co-monomer employed (used in a proportion of 100-x wt.%, not indicated), cat1 is catalyst 1, n is the wt.% of catalyst 1, cat2 is catalyst 2, m is the wt.% of catalyst 2. An example would be S2MA-50_PEGMA_DBN1_TBP2 with means 50% of S2MA, 50% of PEGMA plus 1 wt.% of DBN and 2 wt.% of TBP.

All the formulation contained 2 wt.% of TPO (radical photoinitiator) and 0.25 wt.% of LUP (radical thermal initiator). With regards to the catalyst, different proportions around 0,5-1-2 wt.% of only base, only phosphine or both at the same time were tested.

Firstly, HEA and HEMA were used but after few tests were discarded. Most of the experiments were made using formulations with PEGMA. Nevertheless, as the material did not achieve the desired thermomechanical properties, other methacrylate co-monomers such as IMA and FEMA were analyzed as well.

The liquid formulations were injected into rectangular mold made with two microscope slides subjected with tweezers, with a spacer made of Teflon of 1 mm of thickness with the desired shape. The samples were photocured by irradiation 3 minutes on each side in an Asiga Flash UV chamber. In order to ensure complete curing, they were later UV-postcured for 15 minutes in a Photopol Vacuum UV oven.

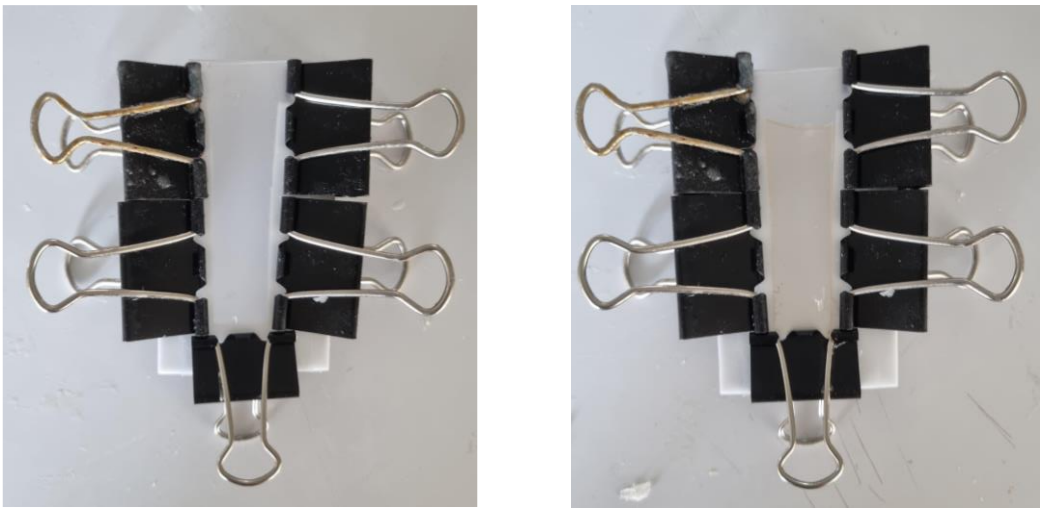

Figure 13: Example of sample preparation

With the purpose of testing the 3D-printing ability of these systems, formulation S2MA-25_FEMA_DBN2 was used. The composition of this formulation is shown in **Error! No s'ha trobat l 'origen de la referència.**.

Table 6: Composition of the S2MA-25_FEMA_DBN2 formulation.

Name	% Weight	Description
S2MA	25	Monomer
FEMA	75	Reactive diluent
TPO	2	Photoinitiator
DBN	2	Catalyst
LUP	0,25	Thermal initiator

The printing process was carried out in an Asiga MAX 3D-printer. The mixture was placed inside the vat and then polymerized layer-by-layer with a resolution of 100 µm in the z direction using a convenient exposure, previously calibrated. The printed samples were washed in isopropanol and later postcured for 30 minutes in a Photopol Vacuum UV oven.

5.4 Instrumentation

Fourier Transform Infrared Spectroscopy (FTIR)

A Brucker Vertex 70FTIR spectrometer equipped with an attenuated total refection (ATR) accessory which is temperature controlled was used to monitor the conversion of the preparation of both monomers S2MA and AzMA. Spectra were collected at room-temperature in absorbance mode with a resolution of 4 cm^{-1} and a wavelength range from 600 to 4000 cm^{-1}, averaging 20 scans for each spectrum. The collected spectra were analyzed using the OPUS software. Different signals were monitored in order to determine the completion of the different reactions: 908 cm^{-1} (epoxy group), 1637 cm^{-1} (methacrylate double bond), 1650 cm^{-1} (carboxyl), 1720 cm^{-1} (carbonyl ester), 3500 cm^{-1} (hydroxyl group).

Differential Scanning Calorimetry (DSC)

A Mettler DSC3+ calorimeter equipped with an intra-cooler was used for the determination of the glass transition temperature (T_g) of the cured materials. Samples of approximately 10 mg were placed in aluminium pans with pierced lids and analyzed at 10 ^oC/min under nitrogen atmosphere. Two scans were performed, the first one to erase the thermal history. The T_g was determined from the second scan as the halfway point in the heat capacity step using the ISO method from the STARe software.

The Mettler DSC3+ was also used to determine the evolution of T_g during thermal treatment of the cured materials at different temperatures. Samples of approximately 10 mg in pierced aluminium pans were kept at prescribed times at a given temperature (80, 100, 120 or 140 ^oC) and the T_g was determined from a subsequent dynamic scan at 10 ^oC/min.

A Meltter DSC821e with a Hamamatsu Lightnincure LC5 (Hg-Xe lamp) with two beams, one for the sample side and the other for the reference side. Samples of liquid uncured formulation of approximately 5 mg cured in open aluminium pans under N2 atmosphere. Two scans were performed on each sample to subtract the thermal effect of the UV irradiation from the photocuring experiment. Samples are photocured at 30 ^oC with the following program: 1 min of temperature conditioning, 10

min of irradiation and finally, 1 min more without UV light, with a lamp diaphragm opening of 10%. After the UV-curing process, the pans were closed with a pierced lid and analyzed in the DSC3+ at 10 ^{o}C/min in order to determine the T_g and the presence of residual heat.

Thermogravimetric analysis (TGA)

Thermogravimetric analysis was carried out with a Mattler TGA/DSC 1 thermobalance with a gas controller GC 200. Samples of approximate mass of 10 mg were degraded between 30 and 800^{o}C at a heating range of 10^{o}C/min in a nitrogen atmosphere (50 ml/min measured in normal conditions). The thermal stability of the cured samples was also analyzed under isothermal conditions at the temperatures of 80, 100, 120, 140 and 160 ^{o}C.

Dynamic mechanica analysis (DMA)

A TA instrumernts DMA Q800 device was used for the determination of the T_g of the cured materials, for the analysis of the stress relaxation of cured samples at different temperatures, and for the mechanical testing of samples.

The T_g was analyzed using a single cantilever clamp at a frequency of 1Hz and 0,05% strain and a heating ramp of 3 ^{o}C/min. Sample dimensions were 10 x 10 x 1 mm^3 (free length x width x thickness). This experiment produced storage modulus (E'), loss modulus (E'') and tan δ (E''/E') signals. The T_g was determined from the temperature of the tan δ peak corresponding to the α-relaxation of the material.

Stress relaxation was performed using a 3-point bending clamp with a preload force of 0,01 N and 1 % strain. Sample dimensions were 20 x 10 x 1 mm^3 (free length x width x thickness). Samples were heated at 10 ^{o}C/min up to the desired temperature and stabilized at that temperature, held isothermally for 5 min prior to the application of the strain and measurement of the stress. Stress relaxation experiments were carried out at 80, 100, 120, 140 and 160 ^{o}C. The relaxation modulus E (MPa) was normalized with respect to the initial modulus E_0 (MPa), therefore the evolution of the dimensionless normalized relaxation modulus E/E_0 was used to assess the rate of stress relaxation.

Mechanical tests were performed using a 3-point bending clamp with a preload force of 0,01 N and a force ramp of 3 N/min and at 25 ^{o}C. Sample dimensions were 20 x 10 x 1 mm^3 (free length x width x thickness).

3D printer

An Asiga MAX UV 385 desktop 3D printer was used to print the different samples for mechanical analysis, assembly/shape memory demonstration test and some decoration pieces. Prismatic rectangular geometries were designed using FreeCAD software and exported in STL file format. Other pre-designed STL files were used for demonstration of printing capabilities. Average wavelength of irradiation was 385 nm, with an irradiation intensity of 6 mW/cm^2. Layer thickness was fixed at 100 µm. Each layer received an irradiation of 136 mJ/cm^2 the first layer and 68 mJ/cm^2 the rest, which was an optimal dose as per calibration results. Samples were washed in isopropyl alcohol after printing, dried, and postcured in a Photopol Vacuum UV chamber with a spectrum ranging between 320nm and 450nm with an irradiation power of 485mW/cm2

Proton nuclear magnetic resonance (^{1}H-NMR)

^{1}H NMR spectra were registered in a Varian VNMR-S400 NMR spectrometer. $CDCl_3$ was used as the solvent. All chemical shifts are quoted on the δ scale in parts per million (ppm) using residual protonated solvent as internal standard (^{1}H NMR: $CDCl_3$ = 7.26 ppm).

6 RESULTS AND DISCUSSION

6.1 Preliminary characterization of the stress relaxation behavior

A preliminary analysis of the effect of the type of catalyst and concentration on the vitrimeric character of this new family of materials was carried out. Formulations containing 50 wt.% of S2MA monomer and PEGMA as co-polymer (S2-50_PEGMA) were selected after a set of trial-and-error experiments. The results of this analysis were compared with those making use of comparable formulation containing AzMA monomer and PEGMA in the same proportions. Tertiary amine and phosphine catalysts were selected because of their known role in disulfide exchange process.[7], [9], [10], [13] The vitrimeric character of these materials was characterized by means of stress-relaxation experiments using DMA, which were carried out at 160°C to accelerate the process.

Figure 14 shows the effect of different types of catalysts (tertiary amines, phosphines) in the relaxation dynamics of materials containing S2MA. The normalized relaxation modulus, E/E_0, is plotted with respect to time in a logarithmic scale. To begin with, it was observed that the material without catalyst could show some residual relaxation, possibly due to the activation of thermal radical dissociation mechanism[6], [8] or else due to the activity of the catalyst used in the preparation of the S2MA monomer. Different tertiary amine catalysts were added in a proportion of 2 wt.%. From the results in Figure 14 , it can be observed that the activity of the different catalysts follows this trend: DBN > TBD = DMAP > TEA > BDMA. The analysis of the phosphine catalyst revealed that 1 wt.% of TBP produced a negligible effect compared with the material without added catalyst, while 2 wt.% of catalyst produced a moderately positive effect, only compared to 2 wt.% of BDMA or TEA, the less effective ternary amine catalyst.

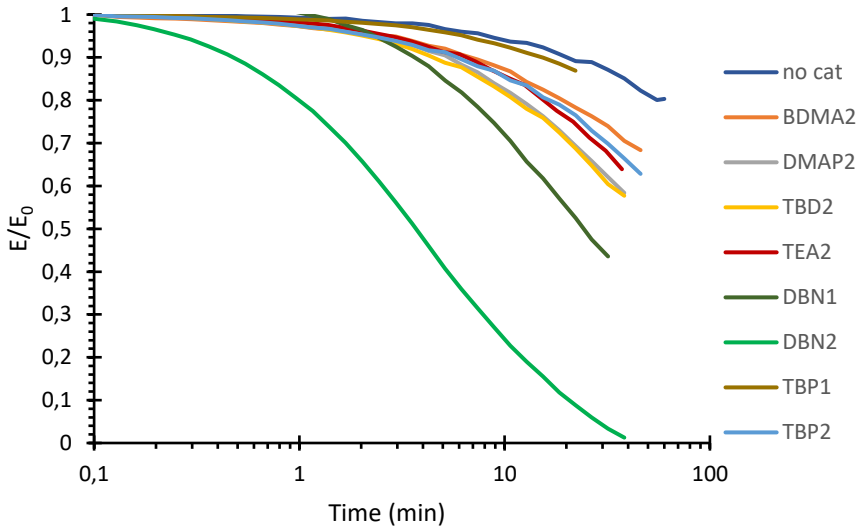

Figure 14: Comparative plot stress-relaxation of different type of catalyst at 160°C.

It was also tried to use a combination of amine (DBN) and phosphine (TBP or TPP). In Figure 15 in can be observed that the addition of TBP and TPP to formulations containing 1 wt.% of DBN produce an acceleration of the relaxation process, but the effect is only moderate by comparison with the material containing 2 w.t% of DBN.

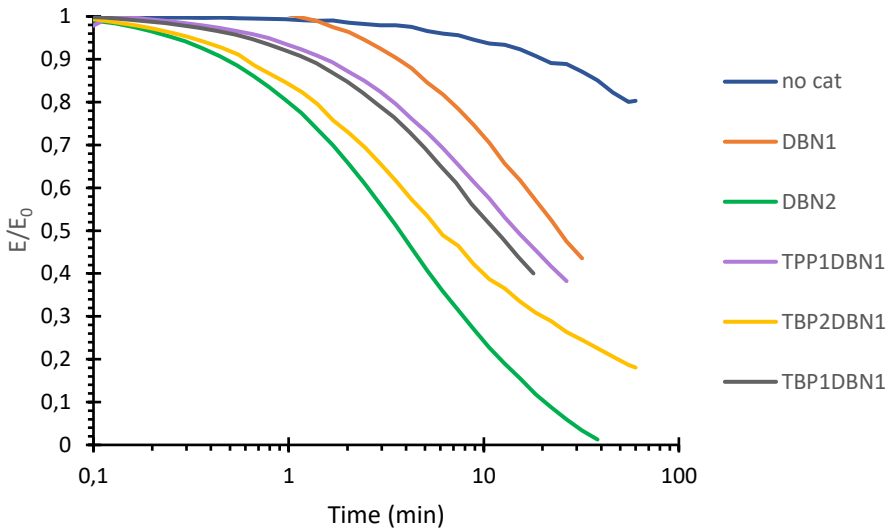

Figure 15: Comparative plot stress-relaxation of different type of catalyst at 160°C

In consequence, it can be observed that 2 wt.% DBN stands out above the rest of the catalysts, providing the best results. Another valid alternative could be 2 wt.% of TBP with 1 wt.% of DBN, but this alternative was not further considered because of the simplicity of the use of just 2 wt.% DBN.

Different mechanisms have been proposed for the base and phosphine-catalyzed disulfide exchange[7], [9], [16]. No tests were carried out to elucidate the exact reaction mechanism. However, solubility tests in DMSO evidenced that the material is not soluble, suggesting that the dynamic bond exchange process follows an associative mechanism.

In order to clarify the effect of the catalyst on the relaxation behaviour, a similar study was carried out on formulations containing AzMA instead of S2MA, in the same proportion. Figure 16 shows that the different catalysts can also produce relaxation of the stress, but to a lesser extent that in formulations containing S2MA. This indicates that these same catalysts can aldo promote dynamic exchange by transesterification involving β-hydroxyesters moieties present in AzMA monomers but also in S2MA. The one without catalyst was not include since it is negligible.

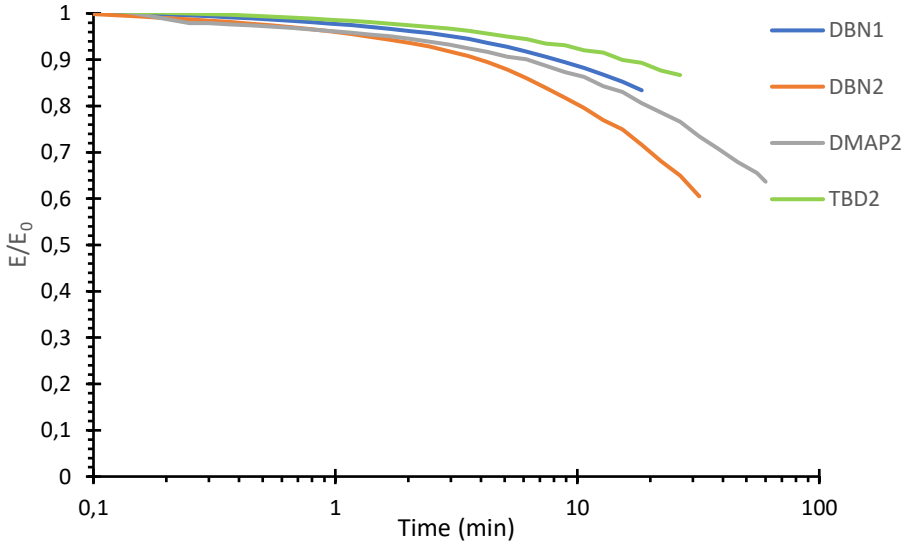

Figure 16: Comparative plot stress-relaxation with AzMA of different type of catalyst at 160°C.

In consequence, it can be assumed that S2MA materials are able to relax stress by two different mechanisms, a dynamic exchange process between disulfide bonds, and transesterification. However, it is also apparent that the former plays a more relevant role.

At this point, having chosen the catalytic system, every formulation will contain 2 w.t% of TPO as the photoinitiator plus 2 w.t% of DBN as a catalyst and therefore will not be include in the nomenclature hereinafter.

6.2 Preliminary analysis of the acrylate/methacrylate composition

In order to define a set of materials for further analysis, it was decided to analyse the effect of the monomer composition on the properties of the material. A series of materials containing different proportions of S2MA and different acrylates and methacrylates were prepared. Table 7 shows that the starting S2-50_PEGMA material has a T_g of -10 ^oC, and that increasing the content of PEGMA further decreases the value of T_g, due to the decrease in the crosslinking density and the high mobility of the polyethylene glycol side chain of the PEGMA monomer. Given the low values of T_g, it was considered that the composition should be changed for the application into 3D-printing.

When PEGMA was fully replaced by HEMA, the resulting T_g was much higher. Combination of HEMA with HEA or PEGMA led to materials with moderate values of T_g. It was attempted to include IMA on the formulations, but that resulted poorly defined T_g. Finally, it was seen that the use of FEMA produced a well-defined T_g slightly above room-temperature, regardless of the amount of FEMA. Both FEMA and IMA possess a bulkier and less mobile side chain, hence the higher T_g in comparison with PEGMA materials. However, the quality of the materials with IMA was worse because of its higher fragility and some compatibility issues resulting in a broad and ill-defined glass transition. Therefore, FEMA was considered as a suitable candidate for further analysis.

Table 7: Different T_g from materials based on S2MA with different proportion and co-monomers determined by DSC.

Name	T_g (^oC)
S2-50_PEGMA	-10
S2-25_PEGMA	-38
S2-50_HEMA	79
S2-25_HEMA_PEGMA	24
S2-25_HEMA_HEA	36
S2-50_PEGMA_IMA	30-50
S2-25_FEMA	40
S2-50_FEMA	40

Additional tests were carried out in order to compare the effect of the (meth)acrylate co-monomer in the stress relaxation behaviour Figure 17 shows only the stress-relaxation tests of the materials containing PEGMA/IMA_PEGMA/FEMA as co-monomer, showing comparable behaviour. In contrast, materials containing HEMA and/or HEA showed a very poor relaxation behaviour (not shown in the Figure 17), which could be explained by the interaction of the hydroxyl groups of the co-monomer and the catalyst.

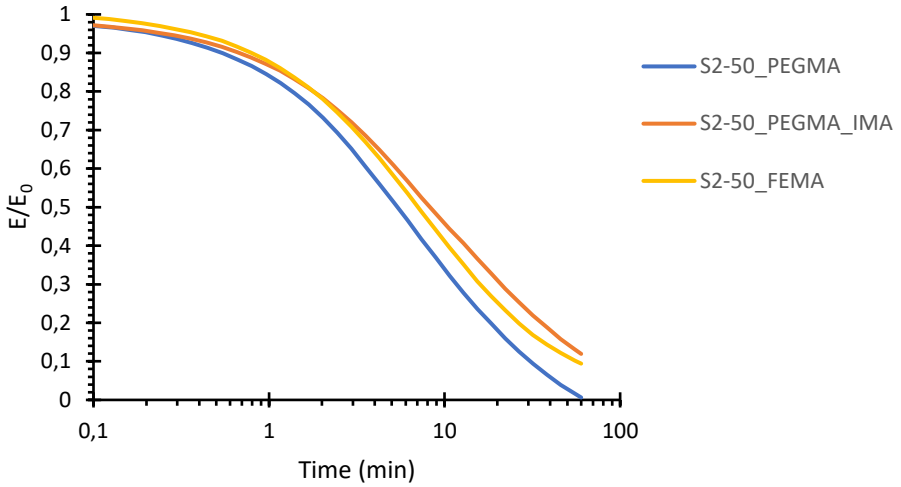

Figure 17: Comparative plot stress-relaxation of S2MA with different co-monomers, 2 wt.% of DBN, at 160°C

As far as relaxation time concerns, S2-50_PEGMA takes less time to relax, but S2-50_FEMA has better thermal-mechanicals properties with an acceptable relaxation time. Given these considerations, it was decided to continue the analysis with FEMA as co-monomer, using only 25 wt.% of S2MA (S2-25_FEMA_DBN2 formulation).

6.3 Study of material based on FEMA co-monomer

Materials with 25 wt.% of S2MA or AzMA and FEMA as reactive diluent, 2 wt.% of TPO as radical photoinitiator, and 2 wt.% of DBN as dynamic bond exchange catalyst were prepared and analyzed using DMA at different temperatures. Both materials have similar structure and glass-transition temperature, as shown in Table 9.

Figure 18 shows that both materials are able to undergo stress relaxation at different temperatures. However, it is overobserved that the relaxation of S2-25_FEMA material is much faster than that of Az-25_FEMA, in a similar way to previous preliminary analysis. This can be explained because of the presence of the β-hydroxyesters bonds in both AzMA and S2MA monomers, which enable both materials to undergo dynamic bond exchange by transesterification reaction. However, the presence of disulfide bonds in S2-25_FEMA, results in a faster relaxation due to the effects of the disulfide exchange reactions.

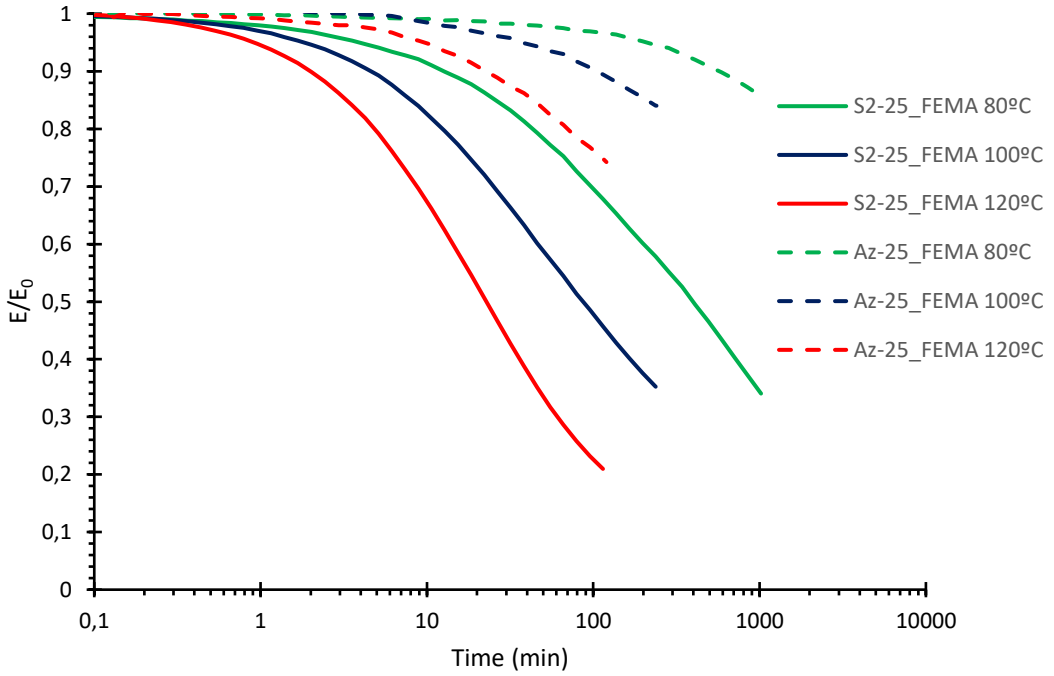

Figure 18: Stress relaxation analysis of S2-25_FEMA and Az-25_FEMA samples carried out at different temperatures.

In addition, the relaxation of S2-25 is comparatively faster than Az-25 with decreasing temperatures, which means that apparently at low temperatures the S-S exchange is promoted with respect to the transesterification. Table 8 compares the time that the different materials take to achieve 15% of relaxation $t = (E = 0.85\ E_0)$. If both values are divided it can be evaluated how S2-25 relaxes comparatively faster at lower temperatures.

Table 8: Comparison of the time needed for the relaxation to 85% of the original stress for S2-25_FEMA and Az-25_FEMA materials at different temperatures.

$t_{E/E0=0.85}$ (min)			
T (℃)	**S2-25**	**Az-25**	**ratio Az/S2**
120	3.3	43.6	13.2
100	8.1	211.3	26.1
80	26.0	1012.2	38.9

Moreover, in Table 9 it is compared the evolution of the T_g of the different materials under thermal treatment at the temperature of 120ºC. The starting value is very similar for both materials, confirming that they are very similar in structure and thermomechanical properties. However, the T_g of Az-25_FEMA material rises 4 degrees after 30 minutes of treatment, while the T_g of the S2-25_FEMA material remains stable. As it has been mentioned before in the monomer preparation, AzMA did not react completely. For this reason, it is speculated that the first rise in T_g (between 0-30min) is because of some additional side reaction takes place when exposed to elevated temperatures.

Table 9: Values of T_g of S2-25_FEMA and Az-25_FEMA after a thermal treatment at 120 ^oC determined by DSC.

	S2-25_FEMA	Az-25_FEMA
Time	**T_g (^oC)**	**T_g (^oC)**
0	44	43
30	48	43
60	49	44
120	49	43

Another way to evaluate T_g is using DMA (Figure 19). The tan δ peak corresponds to the mechanical relaxation of the material associated with the T_g. As it can be noticed, both T_gs are very close, like the storage modulus, reinforcing the idea that S2-25_FEMA and Az-25_FEMA are very similar in structure and thermomechanical properties. The relaxed modulus of the Az-25_FEMA material is apparently higher than that of S2-25_FEMA, suggesting that the crosslinking density would be higher, but this difference was due to experimental error due to the very low stiffness of the material once it is relaxed, below the sensitivity limits of the equipment.

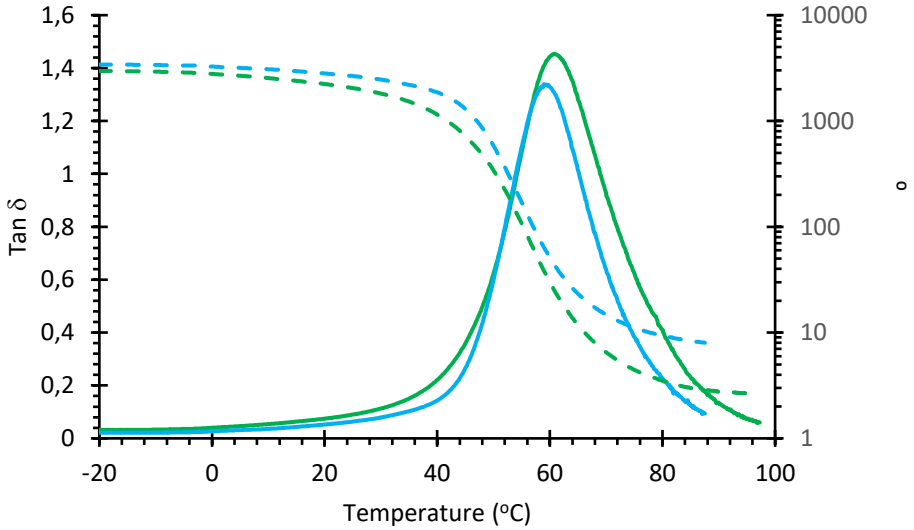

Figure 19: S2-25 has been represented in green colours whereas Az-25 in blue colours. In discontinous line the storage modulus and in solid line Tan Δ

6.4 Effect of the proportion of S2MA

The effect of the proportion of S2MA in formulations containing FEMA was evaluated. Table 10 shows the value of the T_g of the materials containing 25, 50 and 75 wt.% of S2MA. The DSC traces of the glass transition temperatures analysis are also shown in Figure 20. It can be observed that, regardless of the S2MA content, materials with a T_g around 40-45^oC are obtained, in contrast with the results of the preliminary analysis using PEGMA as co-monomer (Table 7). If the structure of the materials is interpreted as copolymer of FEMA (or PEGMA) and S2MA, this means that the T_g of the FEMA homopolymer is very close to that oh the S2MA homopolymer, while the T_g of PEGMA homopolymer

was much lower. This can be rationalized by the different structure of FEMA, having a smaller and bulkier, less mobile side chain than PEGMA, therefore leading to a material with higher T_g.

Table 10: Values of T_g of the cured S2-X_FEMA materials determined by DSC.

Material	T_g (C^o)
S2-25_FEMA	40
S2-50_FEMA	40
S2-75_FEMA	43

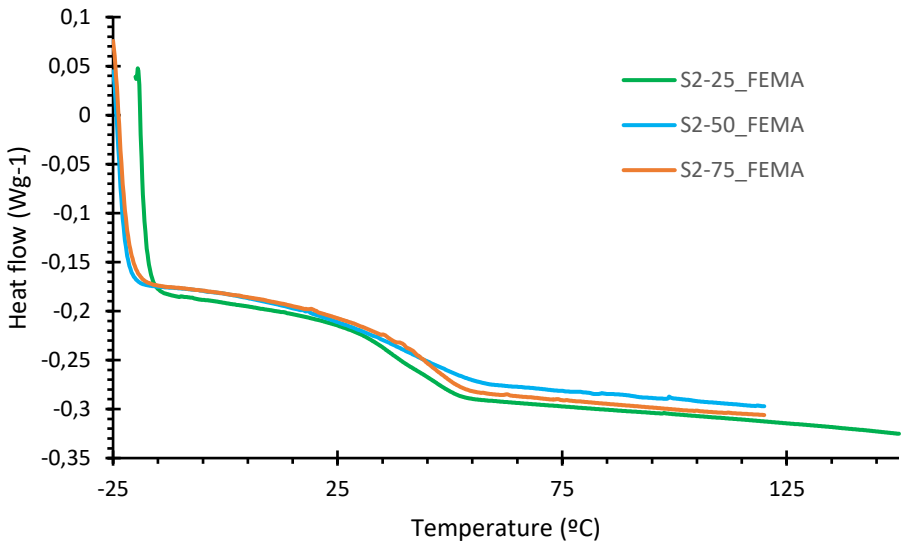

Figure 20: T_g of the S2-X_FEMA materials

Figure 21 shows that as the quantity of S2MA increases, the material takes more time to relax, even though it still behaves as a vitrimer. The reason is that in S2-75_FEMA the network is denser, thus creating mobility restrictions and hindering the reaction.

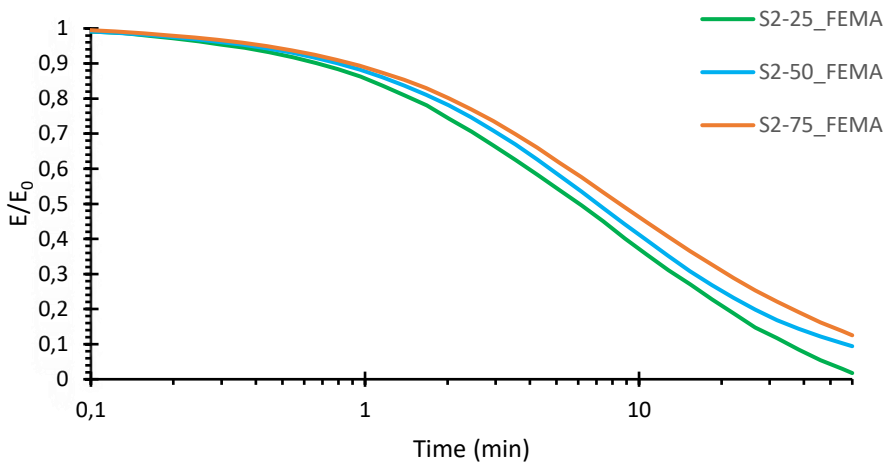

Figure 21: Stress relaxation at 160°C of S2-X_FEMA materials

For the same reason, as S2-75_FEMA has a denser network it is more stable and suffers less changes in its chemical structure. The TGA shown in Figure 22 was carried out under isothermal conditions at 160°C to properly appreciate the difference between each formulation.

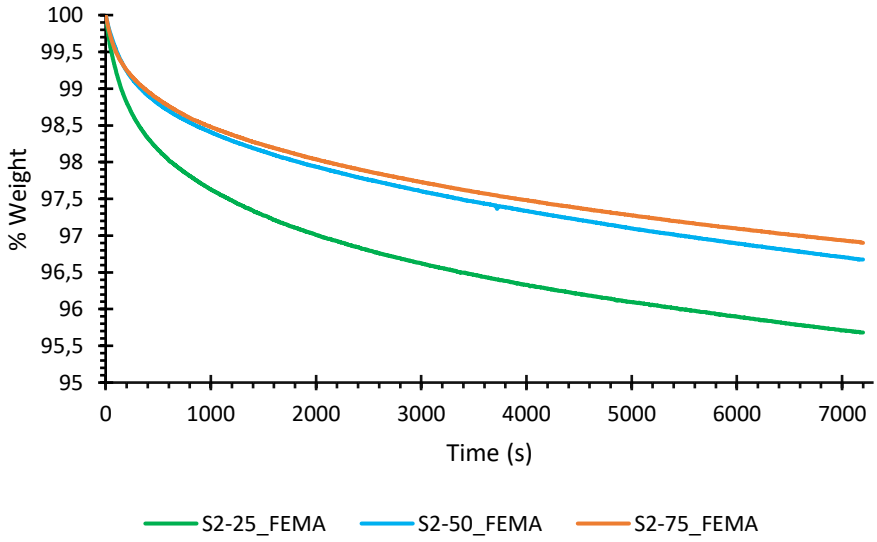

Figure 22: Weight loss duriong isothermal treatment at 160°C of S2-X_FEMA materials

Taking everything into consideration, S2-25_FEMA-DBN2 was the chosen formulation since it behaves as a vitrimer, usually has a short relaxation time and has appropriate thermomechanical properties. In addition, having less quantity of S2MA means that total economic cost is reduced, since the synthesis of this monomer is the most expensive part especially due to the price of 4,4'-dithiodibutyric acid.

6.5 Stress relaxation kinetics analysis

Temperature plays a fundamental role in DMA strain-relaxation analysis and the further research related with reprocessing and recycling. At higher temperatures, the material relaxes faster but can suffer from a loss in mechanical properties or weight.

The kinetics and properties of the S2-25_FEMA_DBN2 were evaluated at different temperatures (80-100-120-140). To obtain an overview about the different changes the material suffers, three kinds of analysis were carried out.

DMA stress-strain analysis was used to measure the relaxation time. As it was expected, the higher the temperature was, the faster the relaxation process is, as seen in Figure 23. However, it is noticed a strange behaviour at the temperature of 140°C, which can be attributed to possible changes taking place in the structure of the material upon thermal treatment at elevated temperatures.

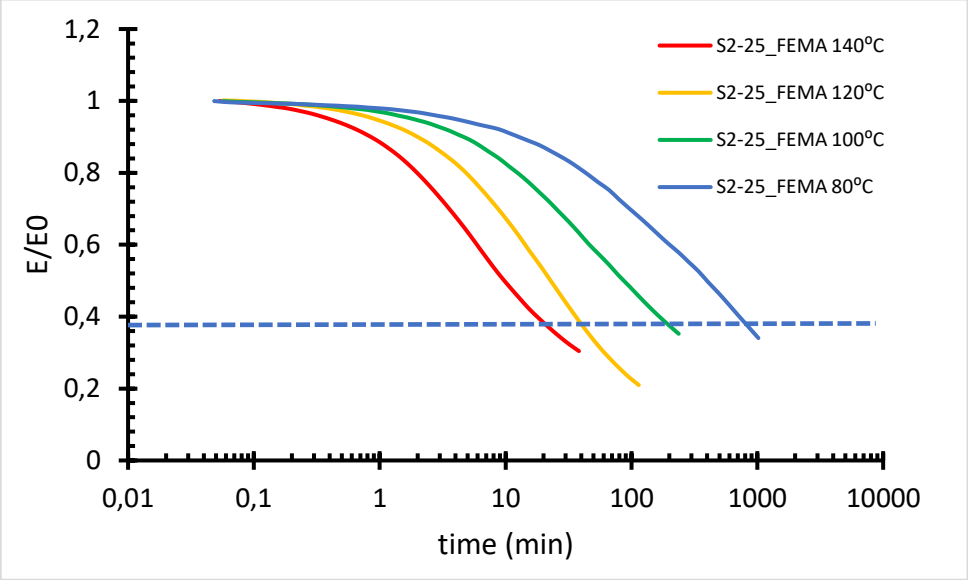

Figure 23: Comparison of the time S2-25_FEMA requires to achieve 0,37 relaxation at different temperatures

The vitrimer relaxation is commonly modelled using a sample Maxwell relaxation model[17] , a single spring with constant G_0 (shear modulus of the material, equivalent to the equilibrium shear modulus of the relaxed material) in series with a dashpot with a viscosity η (representing the ability of the material to relax). Constitutive equations for the Maxwell model are:

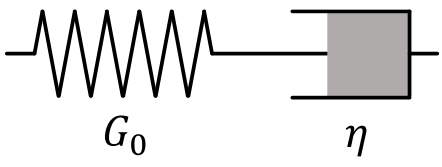

Figure 24: Maxwell model

Equation 1 $$\sigma = G_0 \cdot \varepsilon_E$$

Equation 2 $$\sigma = \eta \cdot \dot{\varepsilon}_\eta$$

Equation 3 $$\varepsilon = \varepsilon_E + \varepsilon_\eta \Longrightarrow \dot{\varepsilon} = \frac{\dot{\sigma}}{G_0} + \frac{\sigma}{\eta}$$

Where σ is the stress and ε is the strain.

For the Maxwell model, the relaxation modulus under constant strain ($\dot{\varepsilon} = 0$) can be expressed as:

Equation 4 $$G = G_0 \cdot exp\left(-\frac{t}{\tau}\right)$$

Where τ is the relaxation time, with $\tau = \eta / G_0$.

For a creep experiment (under constant stress, $\dot{\sigma} = 0$), the viscosity of the fluid-like behaviour is equal to the viscosity of the dashpot, with $\eta = G_0 \cdot \tau = \sigma / \dot{\varepsilon}$ (the higher the slope of a creep experiment, the lower the viscosity).

In this model, G_0 is assumed to be constant (relaxed network structure) and η has a strong temperature dependence. Taking into consideration that flow of vitrimers is governed by a dynamic bond exchange reaction, the viscosity takes an Arrhenius-like form with

Equation 5 $$\eta = \eta_0 \cdot exp\left(\frac{E_{act}}{R \cdot T}\right)$$

In consequence, the relaxation time τ will also have an Arrhenius-like temperature dependence such as:

Equation 6 $$\tau = \tau_0 \cdot exp\left(\frac{E_{act}}{R \cdot T}\right)$$

According to the relaxation model, when $t = \tau$:

Equation 7 $$G = G_0 \cdot exp\left(-\frac{t}{\tau}\right) = G_0 \cdot 1/e \Longrightarrow G/G_0 = 1/e \simeq 0.37$$

If we determine relaxation time $(G/G_0 = 0.37)$ for different temperatures, it can easily derive the temperature dependence by linear regression.

Equation 8 $$ln\,\tau = ln\,\tau_0 + \frac{E_{act}}{R \cdot T}$$

The topology freezing temperature T_v is defined as the temperature at which the viscosity is 10^{12} Pa·s.[5] It is also reported that it could be determined as the temperature at which the relaxation time is 10^6 s,[18] but that may depend on the type and structure of material. Assuming that the Maxwell model is valid,[17] the T_v is determined as the temperature at which η in the dashpot-spring system is equal to 10^{12} Pa·s, so that $\tau = \eta / G_0 = 10^{12} / G_0$.

We characterize the vitrimeric behavior by means of stress relaxation experiments using DMA with a reduced strain (1% in our case), so that the linear viscoelastic expressions of the Maxwell model hold true. We have analyzed the relaxation in flexural mode (3-point bending, 1.5 mm thickness, 10 mm width, 20 mm length). We assume that the relaxation kinetics do not depend on the mode of deformation so that, $E/E_0 = G/G_0 = exp(-t/\tau)$.

Our relaxation data at 80, 100 and 120 ºC are shown in Figure 23 The dashed line represents $E/E_0 = 1/e \simeq 0.37$. The relaxation times at 80, 100 and 120 ºC are 859, 208 and 42 minutes respectively.

Linear regression leads $\boldsymbol{E_{act} = 86900\ J/mol}$ and $\boldsymbol{\ln \tau_0 = -22.8\ (min)}$, with a fairly good correlation, as seen in Figure 25.

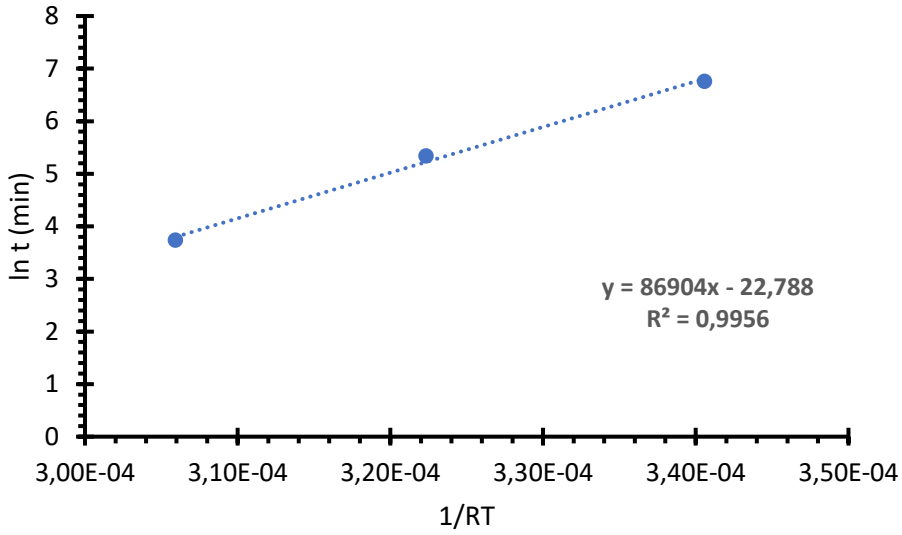

Figure 25: Linear regression used to determine E_{act} and $ln\,\tau_0$

To find the relaxation time at which the viscosity is equal to $\tau = \eta/G_0 = 10^{12}/G_0$ we need a value of the modulus G_0. From the experiments at different temperatures, we have determined experimentally the modulus $E_0 \simeq 4\ MPa$ for the S2-25_FEMA material. Assuming that above the glass transition temperature the Poisson coefficient is $\nu \simeq 0.5$, then

Equation 9
$$G_0 = \frac{E_0}{2\cdot(1+\nu)} \simeq \frac{E_0}{3} = 1.333\ MPa = 1.333 \cdot 10^6\ Pa$$

Then, the relaxation time at the T_v is determined as:

Equation 10
$$\tau = \eta/G_0 = 10^{12}/1.333 \cdot 10^6 = 7.5 \cdot 10^5\ s = 12500\ min$$

Then:

Equation 11
$$ln\,\tau = ln\,\tau_0 + \frac{E_{act}}{R\cdot T}$$

Equation 12
$$T_v = \frac{E_{act}}{R\cdot(ln\,\tau - ln\,\tau_0)} = 324.4\ K = \mathbf{51.3}\ ^{\circ}\mathrm{C}$$

This result indicates that, below approximately 50 °C, the material would behave like a normal thermoset from a practical point of view. It also confirms that the dynamic bond exchange process is very fast, in comparison with typical vitrimer systems based on transesterification processes [5], which have higher T_v. Indeed, comparison of the stress relaxation kinetics with other 3D-printable vitrimer systems[14] shows that the system under study is apparently faster. However, it is also clear that the relaxation process is slower in comparison with other disulfide-based materials [7], [8], [13].

6.6 Thermal stability analysis

Given that the stress relaxation process needs to be carried out at elevated temperatures, it is necessary to analyze if there are changes in the structure and the properties of the materials. In order to do so, the materials were kept under isothermal conditions for prescribed periods of time and their T_g was analyzed using DSC. The results in Table 11 indicate that, at lower temperatures, the materials are highly stable, evidencing very little changes, if any. At elevated temperatures, at 140°C, changes are evident.

Table 11: Values of T_g of S2-25_FEMA at different times and temperatures determined by DSC.

Time (min)	80 °C	100 °C	120 °C	140 °C
0	43	45	43	42
30	-	44	43	44
60	41	44	44	46
120	42	45	43	48
240	43	46	-	-
480	44	-	-	-

This is confirmed by the results of the thermogravimetric analysis of these materials under isothermal conditions. In Figure 26 it can be observed that at higher temperatures the material loses weight at higher rate, being almost negligible at 80°C.

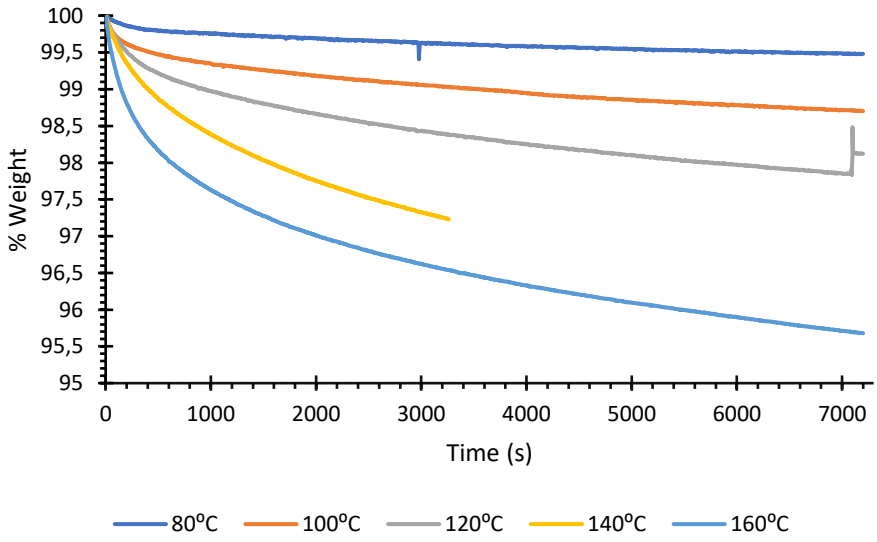

Figure 26: TGA analysis at different isothermal conditions

It is speculated that the decrease in weight may be caused by the loss of volatile fragments, for example molecules that did not react or molecules that contain hydroxyl groups created by transesterification reaction. Some examples are shown in the following schemes.

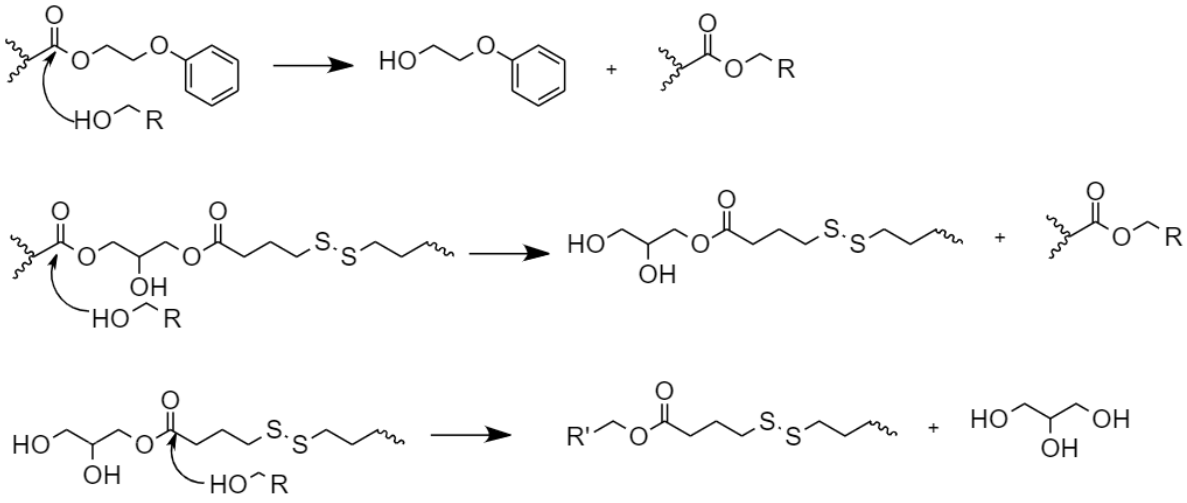

Scheme 6: Possible mechanism for the lost of volatile fragments

These reactions may produce irreversible changes in the network structure of the materials, leading to effective changes in the T_g of the material.

6.7 3D Printing

The other main objective of the project was to test the behavior of the formulation in a 3D Printer. The chosen formulation to be tested has been summed up in Table 12.

Table 12: Composition of the S2-25_FEMA_DBN2 for printing

Component	% Weight	Description
S2MA	25	Monomer
FEMA	75	Reactive diluent
TPO	2	Photoinitiator
DBN	2	Catalyst
LUP	0,25	Thermal initiator

A set of samples was printed to carry out different analyses. UV irradiation time was 8 seconds for the base layer and 6 seconds for the remaining layers. A set of supports had to be created in order to avoid sticking of the sample to the printing platform. After having printed each piece, they were cleaned with isopropanol. Figure 27 shows an example of 3D-printed objects using the formulation under study. Different other pieces with simpler geometries appropriate for testing in the laboratory were also produced.

Figure 27: An example of small pieces done by 3D printer with the chosen material

A preliminary analysis determined that without an appropriate and uniform crosslinking, the analyses are neither reliable or replicable. In consequence, an extended UV irradiation was required in order to ensure complete and uniform degree of cure. For that purpose, 3D-printed samples were UV-postcured for 15 minutes in a Photopol Vacuum UV oven. In consequence, fully-cured samples produced from the 3D-printer were used for the detailed characterization of the S2-25_FEMA materials showed in the previous section.

6.8 Proof of concept

The stress relaxation characteristics of the S2-25_FEMA material was performed in the previous section. In the present section it is only shown the different additional tests that were carried out in order to evaluate the application of this material in repairing and recycling scenarios, which should be possible thanks to the vitrimeric characteristics of these materials.

Repairing ability tests

Tests were carried out in order to see if the dynamic bond exchange chacracteristics of these materials could be used to repair a crack and produce a seamless bonding between the sides of the crack, showing mechanical properties comparable to those of non-cracked materials.

Pieces of 30×10×1,5mm dimensions were cut in half. The pieces were subjected using two blocs and separated about 1 mm. This empty space between the halves was filled with liquid formulation and irradiated with a Hamamatsu LC5 UV-lamp for 1 min. Silicon grease was used to prevent leakage of the low-viscosity liquid below the samples or through the sides. This process was repeated several times to ensure complete filling of the space, making up for the polymerization shrinkage. As well as the printed samples, to achieve a uniform crosslinking they need to remain 15 minutes in a Photopol Vacuum UV oven. Figure 28 illustrates different steps of the repair process.

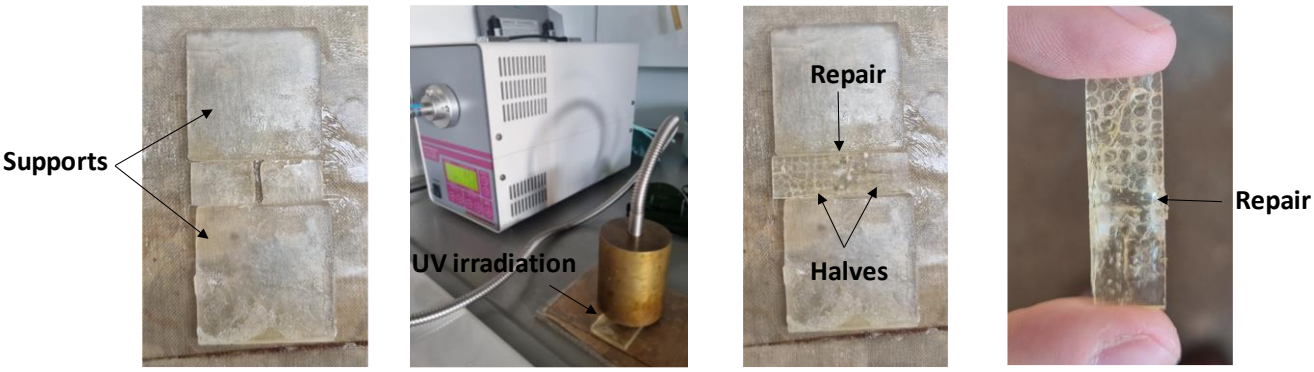

Figure 28: Procedure followed to repair the sample

Once photocured, the samples were put in the oven at different times and temperatures. At 80°C, the samples remain in the oven for 24, 48 and 72h. At 100°C, the samples remained in the oven for 6, 12 and 24h. Finally, at 120°C, the samples remained in the oven for 2, 4 and 6h. In order to ensure the good contact, a light pressure was applied in the longitudinal direction making use of two heavy iron blocks, and a small piece was placed on the sample in order to prevent buckling upwards.

If the repairing process was successful, the mechanical analysis of the repaired samples should produce similar results to those of the original material. Stress-strain analyses at 25 °C using 3-point bending configuration in the DMA were carried out in order to prove the concept. Figure 29 compares the strain-stress curves of different repaired samples in comparison with the original one. It can be seen that the original material has a modulus of 1.7 GPa and achieves 40 MPa of maximum stress. In contrast, none of the repaired samples is successful. The apparent mechanical modulus is similar, but they always break at a lower stress, between 10 and 20 MPa.

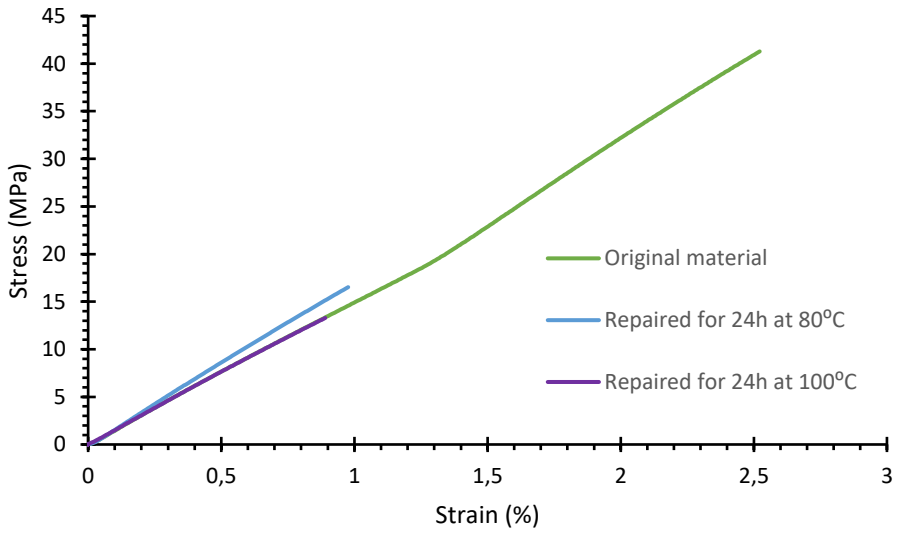

Figure 29: Stress-strain analysis of the repaired materials in comparison with the original.

It was speculated that the reason why none of the samples achieved the original values is because the vitrimer cannot relax its entire network at operating conditions. Moreover, during the repairment process some problems arose, since the pieces do not have a uniform surface there could be some microcracks being already present or appearing in the samples during manipulation and thermal

treatment process. However, it cannot be ruled out that with another process the material could be appropriately repaired.

Analysis of the recycling

The recycling capabilities of the material were tested by hot press moulding of material that was chopped to small pieces, in a similar way to other vitrimeric materials [14], [19]. The chopped material was placed in a mechanical press under 5 tonnes of pressure at 100^{o}C for 24h. Figure 30 shows the resulting sample from that process. The recycling process was apparently successful, but a closer look at the sample revealed that the interface between the chopped samples had not been fully erased in the recycling process, it was visible to the naked eye. The T_g of the material was comparable to that of the untreated material. However, the material was brittle and stress-strain analysis revealed that the elastic modulus was comparable but the material did not resist more than 10-20 MPa, in a similar way to the repaired samples analysed in Figure 29.

Figure 30: Recycled piece from batch 1

It was speculated that the bonds between all the small pieces were not strong enough, so that this recycling process was not valid and more pressure or temperature was required. A second batch was processed at a higher temperature, but the results were equally unsuccessful. Figure 31 shows the resulting sample.

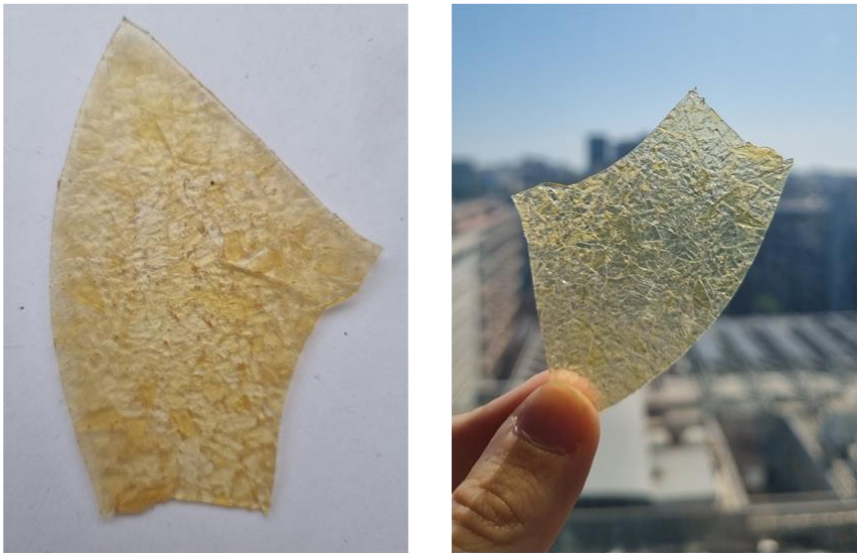

Figure 31: Recycled piece from batch 2

In order to understand the behaviour of these samples, the long-term relaxation of the materials was analysed. In Figure 32 it is observed that the relaxed modulus evolves to a non-zero plateau value, and then the relaxation process continues but at a very slow rate.

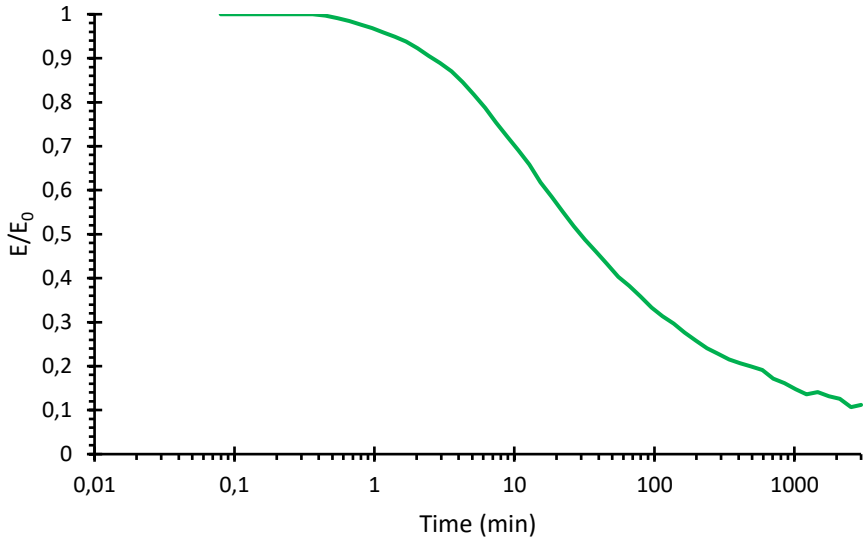

Figure 32: Stress relaxation of S2-25_FEMA at 120^{o}C

This suggests that the structure of the material is changing during the stress relaxation experiment, leading to the formation of a non-relaxing permanent network structure that would prevent the effective recycling and reapairing of the materials.

Indeed, if it is acknowledged that transesterification is taking place in combination with the dynamic bond exchange of disulfides (see Figure 18 from previous section), it is possible to imagine that structures such as the ones seen in Scheme 7 are formed. It can be observed that such the transesterification exchange by the combination of the two species indicated in the scheme would lead to the formation an upper structure in which an additional crosslink would be formed. In addition, for that upper structure the disulfide exchange would not break completely the connection between polymer chains, leading to incomplete stress relaxation. Moreover, a disconnected structure (lower

structure) would be formed, for which the disulfide exchange would be less effective in terms of stress relaxation.

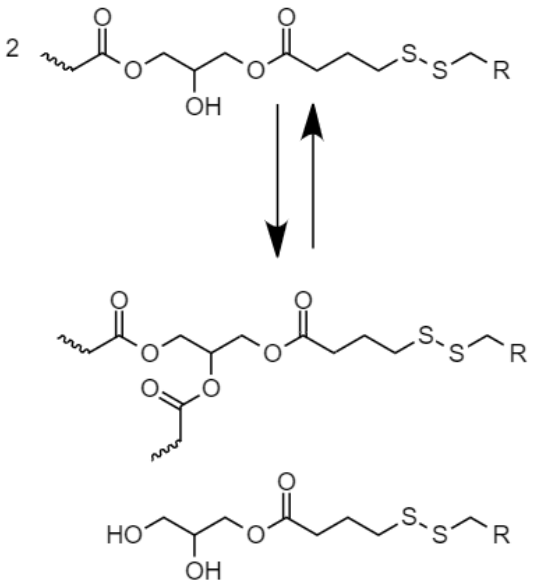

Scheme 7: Possible transesterification of S2MA

The extent to which such structures are formed by transesterification is governed by a temperature-dependent equilibrium[20], which is slowly achieved after curing upon suitable time-temperature conditions. If such structures are formed, then the complete relaxation of the network would require not only fast disulfide exchange but also slow transesterification exchange and therefore a much longer period of time or higher temperature, or both.

If this mechanism is operating, then it poses a relevant drawback to the application of these materials, as they are currently formulated, in terms of their recycling or repairing capabilities. In consequence, it would be necessary to reduce or minimize as much as possible the occurrence of transesterification, or else accelerate the disulfide exchange in a more selective way by choosing suitable catalysts or combinations of them.

7 FURTHER RESEARCH

As it had been mentioned before, 4,4'-dithiodibutyric acid (S2) is an expensive reagent. For this reason, a cheaper acid with S-S bonds was tested, which was the 3,3'-dithiodipropionic acid (S2P). This dicarboxylic acid was used to prepare a dimethacrylate derivative such as the one shown in Figure 33.

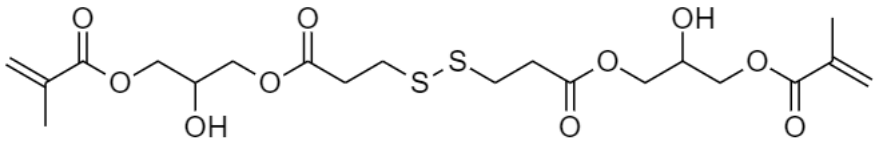

Figure 33: S2PMA

The reaction was carried out in stoichiometric conditions of GMA and S2P, which is equal to 57,48 w.t% and 42,52 w.t% respectively. Different procedures were used for the preparation of the monomers.

The first one was the same procedure used with S2MA. A mixture containing both reagents, plus 0.25 wt.% of TEMPO and 0.25 wt.% of TEA was heated until complete dissolution of the acid, which took place after a few minutes at 110 ^{o}C. Once all the reagents were dissolved, the mixture remained at 100^{o}C for 4 hours with mechanical stirring.

An alternate procedure was based on a different catalyst, triethylamine (TEYA). The first step was to dissolve the acid with GMA and TEMPO at 110^{o}C. After this, TEYA was added (0.25 or 0.5 wt.%) and the mixture was left for 4 hours with mechanical stirring at 100^{o}C.

The prepared monomer, S2PMA, was characterized by FTIR and ^{1}H-NMR. No relevant differences were obtained by FTIR, showing very similar features to the S2MA monomer (see Figure 34 Figure 9: FTIR spectrum of S2MA). The ^{1}H-NMR spectrum (see Figure 35) showed qualitative agreement with the proposed structure although there is a by-product, which possible would be the product obtained by the attack of the acid the more substituted carbon of the epoxide group. This hypothesis can be confirmed by the small signal at 6.1 ppm that integrates 0.51 protons, as well as the signal at 1.85 ppm that integrates 1.86 protons and the small multiplet a 5.2 ppm, which integrates 0.8 protons.

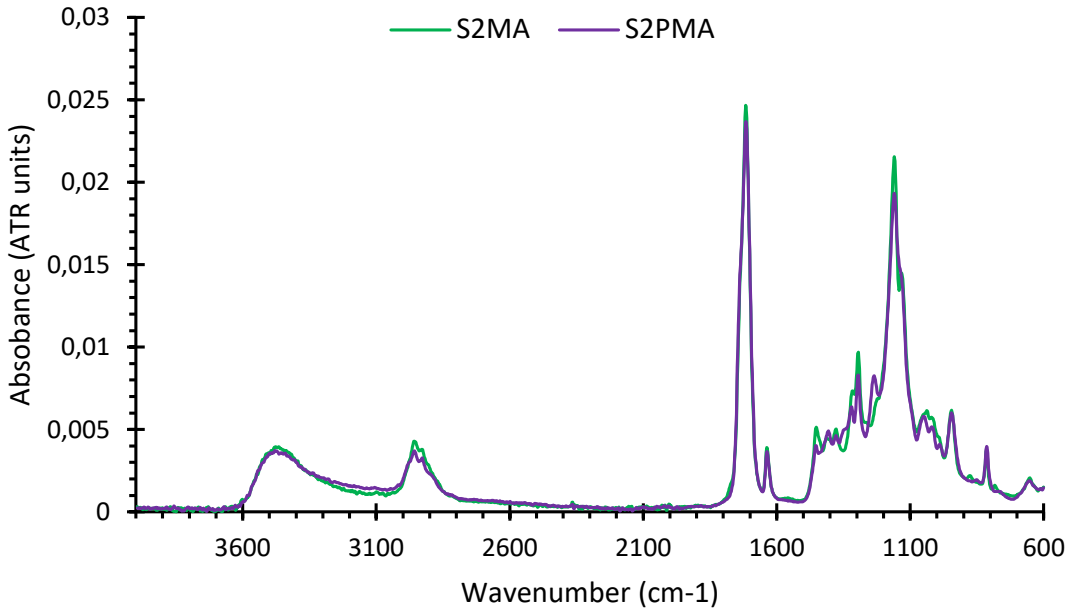

Figure 34: FTIR spectrum of S2MA vs S2PMA

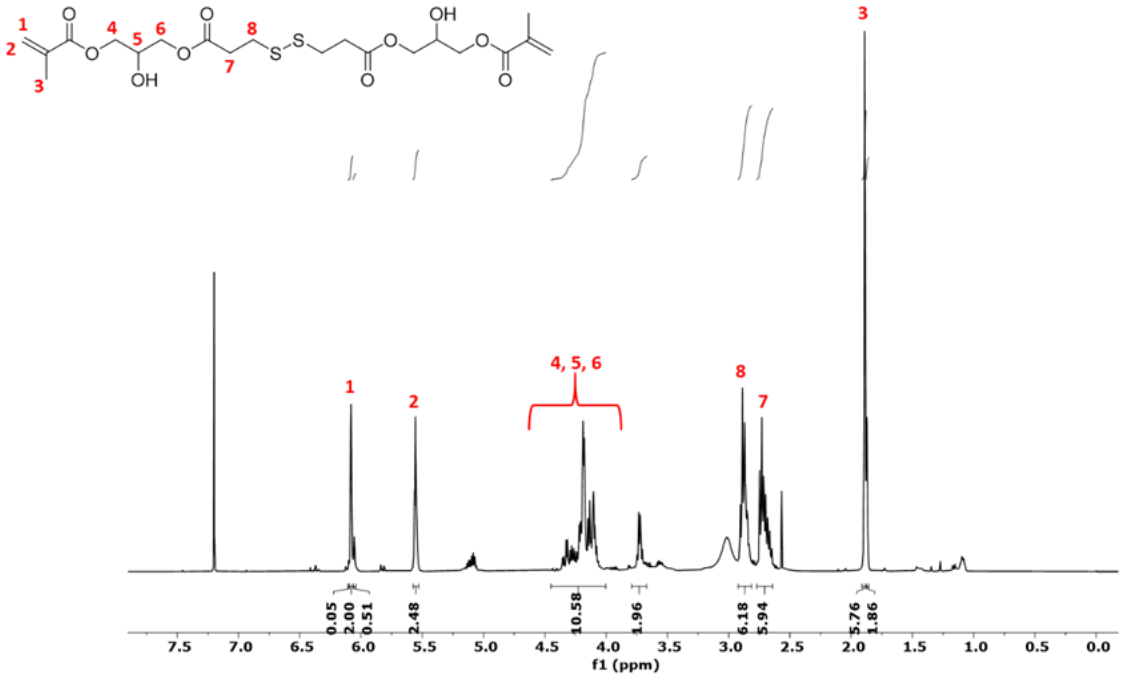

Figure 35_ ^{1}H-NMR spectrum of S2PMA

Materials containing 25 wt.% of S2PMA and FEMA as co-monomer (S2P-25_FEMA) was prepared and characterized, and compared with equivalent material based on S2MA (S2-25_FEMA). The amount of DBN and TPO of the prepared formulations was identical.

The prepared material was characterized by DSC. The results showed that the T_g of S2PMA-based material was about 5^{o}C higher than the material prepared with S2MA, because of the shorter chain of S2PMA, leading to a higher crosslinking density with somewhat less mobile network strands. In general, T_g stands stable in all the tested temperatures, as seen in Table 13.

Table 13: Values of S2P(TEYA)-25_FEMA at different times and temperatures determined by DSC.

Time (min)	80 °C	100 °C	120 °C	140 °C
0	49	49	49	49
30	50	51	52	52
60	50	51	52	52
120	50	51	52	52

Moreover, the thermal stability was analysed using TGA, results shown in Figure 36. Between 80 and 100°C, no difference can be appreciated. The initial weight loss can be related to the possible content of humidity of the material. At higher temperatures, the rate of weight loss increases, as observed in the case of the materials containing the S2MA monomer. Overall, the weight loss is very small, indicating that the materials are highly stable at the temperatures considered for stress relaxation experiments.

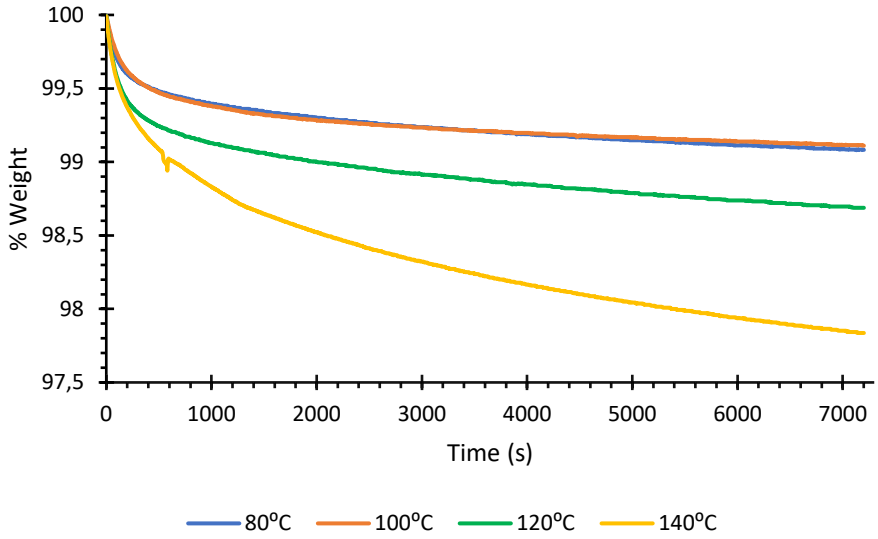

Figure 36: TGA analysis of S2P-25_FEMA material at different isothermal conditions

The stress relaxation of the materials containing S2PMA was also analyzed and compared with that of S2. In Figure 37 it was observed that the relaxation was much faster with S2PMA than with S2MA as it was expected since S2PMA has a higher proportion of S-S bonds. However, it was also observed that the materials could not relax completely, as observed before. In addition, some experimental uncertainties with regards to relaxation behavior of the materials were observed, which make it difficult to extract conclusions regarding the method of preparation of S2PMA monomer.

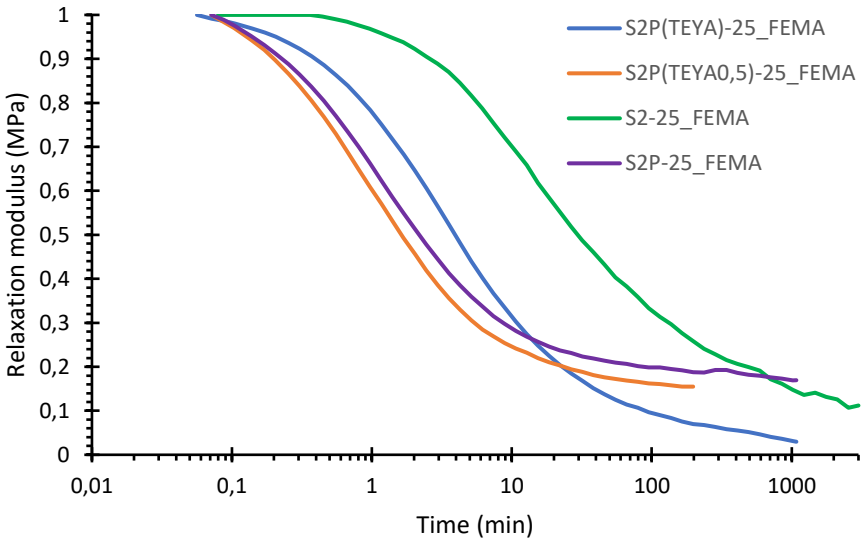

Figure 37: Stress relaxation comparison between S2-25_FEMA and the three formulations with S2P

Materials containing PEGMA instead of FEMA were also tested. In addition, formulations containing 50 wt.% of S2PMA were also prepared. Figure 38 shows that monomers containing 25 wt.% of S2PMA relax faster than materials containing 50 wt.%, suggesting that the mobility of the network structure plays a relevant role in the stress relaxation dynamics. Materials containing PEGMA instead of FEMA also show a faster relaxation behaviour, for that same reason.

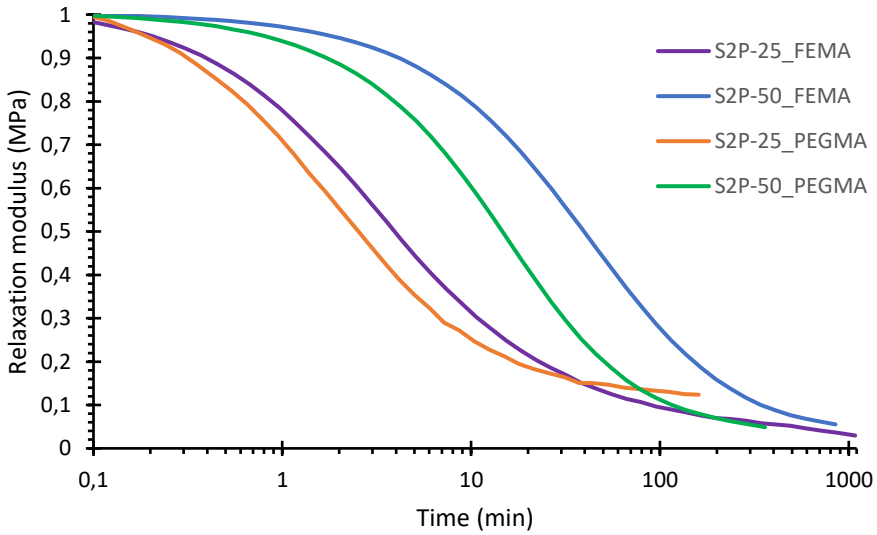

Figure 38: Stress relaxation at 120^{o}C comparison of different formulations with S2P monomer

The fact that the materials do not achieve a 100% relaxation could prevent them from being repaired and/or recycled. Therefore, the exact role of transesterification reactions needs to be analysed in detail.

8 CONCLUSIONS

A new family of vitrimeric materials based on the dynamic exchange of disulfide linkages has been developed.

The initial monomer, S2MA, was prepared without purification or solvents, thus providing an easy and replicable way to prepare it. In addition, a set of analytical techniques were used for its characterization, such as FTIR and ^{1}H NMR. However, it will be necessary to analyze the monomer structure using ^{13}C NMR, a mass spectrometer and chromatography techniques to confir, the identity of thebside products.

All the materials remained stable at work temperatures, ranging from 80 to 160^{o}C, with small weight loss and little changes in their thermomechanical properties at high temperatures. The T_g also stays stable for materials with PEGMA and FEMA along different times and temperatures. It is also worth mentioning that the higher proportion of crosslinking agent (prepared monomer) there is, the more the T_g increases and the more difficult the relaxation is.

An appropriate catalytic system which activates the disulfide bond exchange was found. After evaluating the vitrimeric capabilities of the different materials, the best material formulation was S2MA-25_FEMA_DBN2. DBN can promote both the disulfide exchange and the transesterification process, but the first process is much faster.

The material presents a relax-strain typical from vitrimeric materials, with a $E_{act} = 86900\ J/mol$, which is faster than common transesterification. Moreover, the solubility test, carried out using DMSO, reinforces the idea that the exchange reaction goes through an associative mechanism, which is characteristic from vitrimeric materials.

The selected formulation was tested in the 3D printer and it was able to print samples and small objects. However, the material was not repairable nor recyclable. It is hypothesized that either the procedure was not correct or else that the network relaxation was not complete because of side transesterification reactions taking place, leading to the formation of a permanent network structure with much slower relaxation dynamics. Further research is needed.

In order to improve its large-scale applications, a cheaper monomer (S2PMA) was synthesized. The main problem with this monomer is that it needs to be made at a higher temperature (110^{o}C). Even though the materials made with this monomer show promising results, further research is needed in order to improve the preparation of this monomer, its characterization and its possible applications. The material seems to relax faster than the materials made with S2MA, but they still cannot achieve a complete relaxation. It is speculated that the reason behind this is because it has a permanent network that creates more restrictions and hinders the exchange reaction. This permanent network could be formed during the monomer preparation or else by transesterification taking place during stress relaxation. The subproduct formed by the attack of the carboxylate to the more substituted carbon leads to the formation of a primary alcohol which it is more reactive than a second one. Consequenly, the side transesterification reactions leading to permanent crosslink structures would take place faster. It is therefore necessary to explore new catalysts or combinations of them that enable a more selective activation of the disulfide exchange in order to prevent or minimize the effect of these side transesterification reactions.

CONCLUSIONS

S'ha desenvolupat una nova família de materials vitrimerics basats en enllaços S-S dinàmics.

El monòmer inicial, S2MA, va ser preparat sense cap purificació ni solvents. Això fa possible que la seva preparació sigui senzilla i repetible a nivell tecnològic. A més, es van emprarun seguit de tècniques analítiques per a la seva caracterització com ara FTIR i ^{1}H-RMN. Encara així seria convenient analitzar el monòmer utilitzant ^{13}C-RMN, espectroscòpia de masses i alguna tècnica cromatogràfica per determinar el pes molecular del producte i confirmar la identitat dels productes secundaris.

Tots els materials es mantenen estables a les temperatures de treball, des de 80 fins 160^{o}C, amb petites pèrdues de pes i lleugers canvis en les seves propietats termomecàniques a altes temperatures. La T_g també es mantée estable pels materials amb PEGMA i FEMA al llarg del temps i a diferents temperatures. Val la pena esmentar que quan més agent d'entrecreuament (monòmer preparat) hi ha a la formulación, més alta es la T_g i més dificultat per relaxar té el material curat.

Es va aconseguir un sistema catalític apropiat, el qual activava selectivament el bescanvi S-S. Un cop avaluades les propietats vitrimeriques de diferents materials, es va escollir com a millor la formulació S2MA-25_FEMA_DBN2. El DBN pot activar tant el bescanvi S-S com la transesterificació, però el primer procés es més ràpid.

El material presenta una relaxació-deformació típica de vitrimers, amb una $E_{act} = 86900\, J/mol$, la qual es més ràpida que la ja esmentada transesterificació. A més, es va realitzar un test de solubilitat amb DMSO, el qual va reforçar la idea de que la reacció de bescanvi va via un mecanisme associatiu típic dels vitrimers.

Es va probar la formulación escollida en una impressora 3D, sent capaç d'imprimir petits objectes. Encara així, el material obtingut no és ni reparable ni reciclable. Es pensa que cap d'ambdós processos es va realitzar de forma adient o que la xarxa no es capaç de relaxa completament a causa de la reacció secundaria de transesterificació, donant lloc a una xarxa diferent la qual relaxa més lentament.

Per tal d'optimitzar les seves aplicacions a gran escala, s'ha sintetitzatun nou monòmer més econòmic (S2PMA). El principal problema que presenta es que es requereix més temperatura en la seva síntesis (110^{o}C). Tot i així els materials fets a partir d'aquest monòmer mostren resultats prometedors, però s'ha de seguir investigant per millorar-ne la seva preparació, caracterització i possibles aplicacions. Un exemple d'això es que el material sembla relaxar més ràpid que els materials fets amb S2MA, tantmateix no arriben a una relaxació completa. Pensem que la raó darrera és per que es produeix una xarxa permanent que crea més restriccions i impedeix que es doni la reacció de bescanvi. Aquesta xarxa permanent pot ser formada durant la preparació del monòmer a causa d'especies secunadaries que al ser incorporades a la xarxa dificulten la relaxació d'aquesta o a causa de la reacció de transesterificació que te lloc durant la relaxació-deformació. Per tot això és necessari explorar nous catalitzadors capaços d'activar més selectivament el bescanvi S-S per tal de prevenir o minimitzar els efectes de la reacció secundaria de transesterificació.

9 APPRECIATON

First of all, I would like to thank my directors Xavier Fernández Francos and Xavier Ramis Juan for giving me the opportunity to perform my bachelor's thesis with them and specially for the patience, support and great help that they have provided to me during these months.

Xavier Fernández, thank you for showing me and teaching me in this new field, I enjoyed every day.

Also, I want to thank the rest of the staff in Thermodynamics Laboratory for the help that I have received at some point in my stay in the laboratory.

Likewise, I apreciate Angels Serra Albet for trusting in me and giving me the oportunity to expand my knowledge with this project.

At a personal level, I would like to thank everyone who has supported me and suffered with me, my friends, my university classmates and my family. Thank you for supporting me and helping me through this stage of my life.

What's next?

To be continued...

10 REFERENCES

[1] J.-P. Pascault, H. Sautereau, J. Verdu, and R. J. J. Williams, *Thermosetting Polymers*. New York, 2002.

[2] Q. Shi *et al.*, "Recyclable 3D printing of vitrimer epoxy," *Materials Horizons*, vol. 4, no. 4, pp. 598–607, Jul. 2017, doi: 10.1039/c7mh00043j.

[3] O. Asvany, K. M. T. Yamada, S. Brünken, A. Potapov, and S. Schlemmer, "Experimental ground-state combination differences of CH5+," *Science (1979)*, vol. 347, no. 6228, pp. 1346–1348, Mar. 2015, doi: 10.1126/science.aaa3304.

[4] S. C. Ligon, R. Liska, J. Stampfl, M. Gurr, and R. Mülhaupt, "Polymers for 3D Printing and Customized Additive Manufacturing," *Chemical Reviews*, vol. 117, no. 15. American Chemical Society, pp. 10212–10290, Aug. 09, 2017. doi: 10.1021/acs.chemrev.7b00074.

[5] M. Damien, C. Mathieu, T. François, and L. Ludwik, "Silica-Like Malleable Materials from Permanent Organic Networks," *Science (1979)*, vol. 334, no. 6058, pp. 965–968, Nov. 2011, doi: 10.1126/science.1212648.

[6] W. Denissen, J. M. Winne, and F. E. du Prez, "Vitrimers: Permanent organic networks with glass-like fluidity," *Chemical Science*, vol. 7, no. 1. Royal Society of Chemistry, pp. 30–38, Jan. 01, 2016. doi: 10.1039/c5sc02223a.

[7] Z. Q. Lei, H. P. Xiang, Y. J. Yuan, M. Z. Rong, and M. Q. Zhang, "Room-temperature self-healable and remoldable cross-linked polymer based on the dynamic exchange of disulfide bonds," *Chemistry of Materials*, vol. 26, no. 6, pp. 2038–2046, Mar. 2014, doi: 10.1021/cm4040616.

[8] I. Azcune and I. Odriozola, "Aromatic disulfide crosslinks in polymer systems: Self-healing, reprocessability, recyclability and more," *European Polymer Journal*, vol. 84. Elsevier Ltd, pp. 147–160, Nov. 01, 2016. doi: 10.1016/j.eurpolymj.2016.09.023.

[9] R. Caraballo, M. Rahm, P. Vongvilai, T. Brinck, and O. Ramström, "Phosphine-catalyzed disulfide metathesis," *Chemical Communications*, no. 48, pp. 6603–6605, 2008, doi: 10.1039/b815710c.

[10] S. Nevejans, N. Ballard, J. I. Miranda, B. Reck, and J. M. Asua, "The underlying mechanisms for self-healing of poly(disulfide)s," *Physical Chemistry Chemical Physics*, vol. 18, no. 39, pp. 27577–27583, 2016, doi: 10.1039/c6cp04028d.

[11] X. Li *et al.*, "Self-Healing Polyurethane Elastomers Based on a Disulfide Bond by Digital Light Processing 3D Printing," *ACS Macro Letters*, vol. 8, no. 11, pp. 1511–1516, Nov. 2019, doi: 10.1021/acsmacrolett.9b00766.

[12] E. Rossegger *et al.*, "Digital light processing 3D printing with thiol-Acrylate vitrimers," *Polymer Chemistry*, vol. 12, no. 5, pp. 638–644, Feb. 2021, doi: 10.1039/d0py01520b.

[13] M. Pepels, I. Filot, B. Klumperman, and H. Goossens, "Self-healing systems based on disulfide-thiol exchange reactions," *Polymer Chemistry*, vol. 4, no. 18, pp. 4955–4965, Sep. 2013, doi: 10.1039/c3py00087g.

[14] B. Zhang, K. Kowsari, A. Serjouei, M. L. Dunn, and Q. Ge, “Reprocessable thermosets for sustainable three-dimensional printing,” *Nature Communications*, vol. 9, no. 1, Dec. 2018, doi: 10.1038/s41467-018-04292-8.

[15] L. Li, X. Chen, and J. M. Torkelson, “Covalent Adaptive Networks for Enhanced Adhesion: Exploiting Disulfide Dynamic Chemistry and Annealing during Application,” *ACS Applied Polymer Materials*, vol. 2, no. 11, pp. 4658–4665, Nov. 2020, doi: 10.1021/acsapm.0c00720.

[16] F. I. Altuna, C. E. Hoppe, and R. J. J. Williams, “Epoxy vitrimers with a covalently bonded tertiary amine as catalyst of the transesterification reaction,” *European Polymer Journal*, vol. 113, pp. 297–304, Apr. 2019, doi: 10.1016/j.eurpolymj.2019.01.045.

[17] W. Denissen, G. Rivero, R. Nicolaÿ, L. Leibler, J. M. Winne, and F. E. du Perez, “Vinylogus Urethane Vitrimers,” *Adv Funct Mater*, 2015.

[18] M. Capelot, M. M. Unterlass, F. Tournilhac, and L. Leibler, “Catalytic Control of the Vitrimer Glass Transition,” *ACS Macro Letters*, vol. 1, no. 7, pp. 789–792, Jul. 2012, doi: 10.1021/mz300239f.

[19] F. Gamardella, S. Muñoz, S. de la Flor, X. Ramis, and A. Serra, “Recyclable organocatalyzed poly(Thiourethane) covalent adaptable networks,” *Polymers (Basel)*, vol. 12, no. 12, pp. 1–18, Dec. 2020, doi: 10.3390/polym12122913.

[20] F. I. Altuna, C. E. Hoppe, and R. J. J. Williams, “Epoxy vitrimers: The effect of transesterification reactions on the network structure,” *Polymers (Basel)*, vol. 10, no. 1, Jan. 2018, doi: 10.3390/polym10010043.